Lehigh University
Lehigh Preserve

Fritz Laboratory Reports | Civil and Environmental Engineering

1990

Discretization errors in finite element models of hyperbolic cooling tower shells, May 1990. 63p

Ashfaque Chowdhury

Celal N. Kostem

Follow this and additional works at: http://preserve.lehigh.edu/engr-civil-environmental-fritz-lab-reports

Recommended Citation
Chowdhury, Ashfaque and Kostem, Celal N., "Discretization errors in finite element models of hyperbolic cooling tower shells, May 1990. 63p" (1990). *Fritz Laboratory Reports.* Paper 485.
http://preserve.lehigh.edu/engr-civil-environmental-fritz-lab-reports/485

This Technical Report is brought to you for free and open access by the Civil and Environmental Engineering at Lehigh Preserve. It has been accepted for inclusion in Fritz Laboratory Reports by an authorized administrator of Lehigh Preserve. For more information, please contact preserve@lehigh.edu.

LEHIGH UNIVERSITY LIBRARIES
3 9151 00942809 1

400.40

Lehigh University

DISCRETIZATION ERRORS IN FINITE ELEMENT MODELS OF HYPERBOLIC COOLING TOWERS

FRITZ ENGINEERING
LABORATORY LIBRARY

by

Ashfaque Chowdhury

Celal N. Kostem

Fritz Engineering Laboratory

Fritz Engineering Laboratory Report No. 400.40

DISCRETIZATION ERRORS

IN

FINITE ELEMENT MODELS

OF

HYPERBOLIC COOLING TOWER SHELLS

by

Ashfaque Chowdhury
Celal N. Kostem

FRITZ ENGINEERING
LABORATORY LIBRARY

Fritz Engineering Laboratory

Department of Civil Engineering

Lehigh University

Bethlehem, Pennsylvania 18015

May 1990

Fritz Engineering Laboratory Report No. 400.40

Table of Contents

List of Figures

List of Tables

ABSTRACT

The effect of mesh fineness of finite element models on accuracy of finite element analysis solution is investigated for hyperbolic cooling tower shells. The sensitivity of the errors to geometry of the shell is also examined. Elastic material model and static gravity loading is used.

The study findings indicate that under symmetric state of stress, inadequate mesh fineness may cause significant error in the shell force estimate from finite element analysis. The accuracy of longitudingal shell force estimate is fairly insensitive to the geometry of shell. However even small changes in the shape may drastically affect the accuracy of meridianal shell force estimate.

Chapter 1
Introduction

1.1 Context

Finite Element (FE) mesh characteristics for thin shell continuum problems have traditionally been based on engineering judgement. The effect of mesh fineness and different geometries on the accuracy of the solution is not known. Whether these errors, arising from modelling of the shell are significant or not is an open question.

This study tries to quantify the error in the estimate of shell forces in FE analysis for different mesh refinement levels for the case of a hyperbolic cooling tower shell. The sensitivity of these errors, due to gravity loading, to geometry in this class of shells is also investigated. The material model is elastic and analysis is linear. Error in only gravity loading is considered.

1.2 Literature Survey

There has been substantial research (Rheinboldt, 1985) on error estimation of FE analysis results using different meshes for a given structure, especially for nonlinear problems. However the purpose of these studies were to develop computer programs for automatically generating and adapting finite element meshes, i.e.,"Adaptive FE mesh generation". None of the research focused on specific problems in thin shell analysis. How the different parameters of the mesh itself effect the accuracy of the solution for a particular shell structure was not investigated.

Most studies on FE analysis of hyperbolic cooling tower shells have

concentrated either on the seismic response modelling (Grant, 1980) or on the stresses at the shell-column junction (Iyer, 1990). Though publications on FE modelling (Meyer, 1987) discuss the effects of aspect ratio of elements, little is said about the effects of overall mesh fineness in thin shell problems. The effect of modelling decisions by the analyst (e.g. pattern and fineness of FE mesh, choice of element etc.) on the quality of the solution over the entire shell surface has remained largely unknown.

1.3 Problem Statement and Scope

This study investigates the effect of fineness of FE mesh on accuracy of solution of hyperbolic cooling tower shells of different curvatures. So that more informed decisions about choice of mesh fineness may be made for shells of this type. The error analysis was based on an elastic and static FE model under gravity loading. The scope of this study is limited to examining the relationship of mesh fineness and accuracy of solution in a chosen range of hyperbolic cooling tower shells. Effect of choosing different elements or other ranges of geometric parameters is not investigated. The scope is also limited to elastic material models and symmetric states of stress generated by gravity loading.

Number of divisions in FE mesh in longitudinal (height) and meridianal (radial) directions are taken as the primary variables. Error distribution of FE results for different combinations of these variables are analyzed. Different structural geometries, in this class of shells, are also introduced as a variable. Cost effectiveness of the analysis is also discussed. Based on these results some guidelines for FE modelling of hyperbolic cooling tower shells is sought.

Chapter 2
Methodology

2.1 Overview

For an accurate estimation of errors introduced in FE analysis, a consistent methodology has to be followed. This means a set of definition of stresses and errors has to be established and followed rigorously for each set of analysis results, so that they can be compared.

The following sections each deal with a particular stage of analysis and define the pertinent methods that were used at that stage.

2.2 Finite Element Models

Finite element software package ADINA[1] was used for all the FE analysis in this study. All the FE models used to analyze the hyperbolic cooling tower shells had a number of generic qualities so that the results based on these models could be compared. Also by defining these guidelines a computer program 'CREATE' (Chowdhury, 1990) could be developed, so that the input files required for the FE analysis could be generated automatically. The program is written in C programming language. The program prepares the input files, for the preprocessor ADINA-IN provided with the software package, as well as post-processing and batch job processing files as required, for an entire series of shells.

Usage of the input program not only reduced the manual effort necessary

[1]ADINA is a proprietary software distributed by ADINA R & D, Inc., MA.

for each set of FE analysis, but also ensured that the input files for each case were uniform and free of oversight error. The characteristics which were common to all FE models were as follows.

- Divisions in both radial and height direction of the shells were uniform. The spacing between the divisions were not varied over the entire shell. (See Fig.2-1)
- The bottom of the shell was considered hinged while the top was modelled as free.
- Four noded shell elements were used to model the shell.
- All the nodes in the shell were modelled with 5 degrees of freedom (DOF) except when the surface of the shell elements joining there had an angle exceeding 20^{o} .
- A constant shell thickness of 5 inches was assumed for all the shells.
- Uniform gravity load of 150 psf was considered to be acting.

Uniform divisions in both the directions are used in every FE mesh. So meshes with a higher number of divisions represent a finer mesh. Throughout this study FE mesh sizes are presented as,

*No. of radial divisions * No. of axial divisions*

The cost index was taken as the cost of executing only the FE solution part (ADINA) of the FE package, in batch mode at off hours on a CDC-CYBER computer at Lehigh University Computing Center.

The variation of stresses along the height of the structure was found from the FE analysis and stored for comparison. The results were included in a spreadsheet and the appropriate parts outputted into an ASCII file. Manual re-entering of the data was not necessary at any step, thereby reducing the risk of introducing accidental errors.

2.3 Standard Solution

Classical Solutions for gravity loading on hyperbolic cooling tower shells are available in literature (Soare, 1967) (Ramaswamy, 1986). A numerical integration scheme of this standard solution (See Appendix B) was used as the 'benchmark' solution for estimating errors in the FE solutions. Membrane theory solution which mainly considers the in-plane action of the shell was adopted. Since the structure under gravity load primarily displays an in-plane response, membrane theory provides a very accurate solution. At the ends of the shell where there is some bending action the membrane theory solution may deviate marginally from the actual stresses, but over most of the shell surface the solution may be taken as very close to an 'exact' solution.

2.4 Error Analysis

In the context of this study, error is estimated as the difference between shell forces from membrane theory model and FE solution. Errors are found and plotted along the height for each FE analysis for both axial and radial direction shell forces. (See Appendix A for nomenclature)

$$e_{\phi} = N_{\phi, FE} - N_{\phi, std}$$
$$e_{\theta} = N_{\theta, FE} - N_{\theta, std}$$

A computer program 'ERROR', in PASCAL programming language,

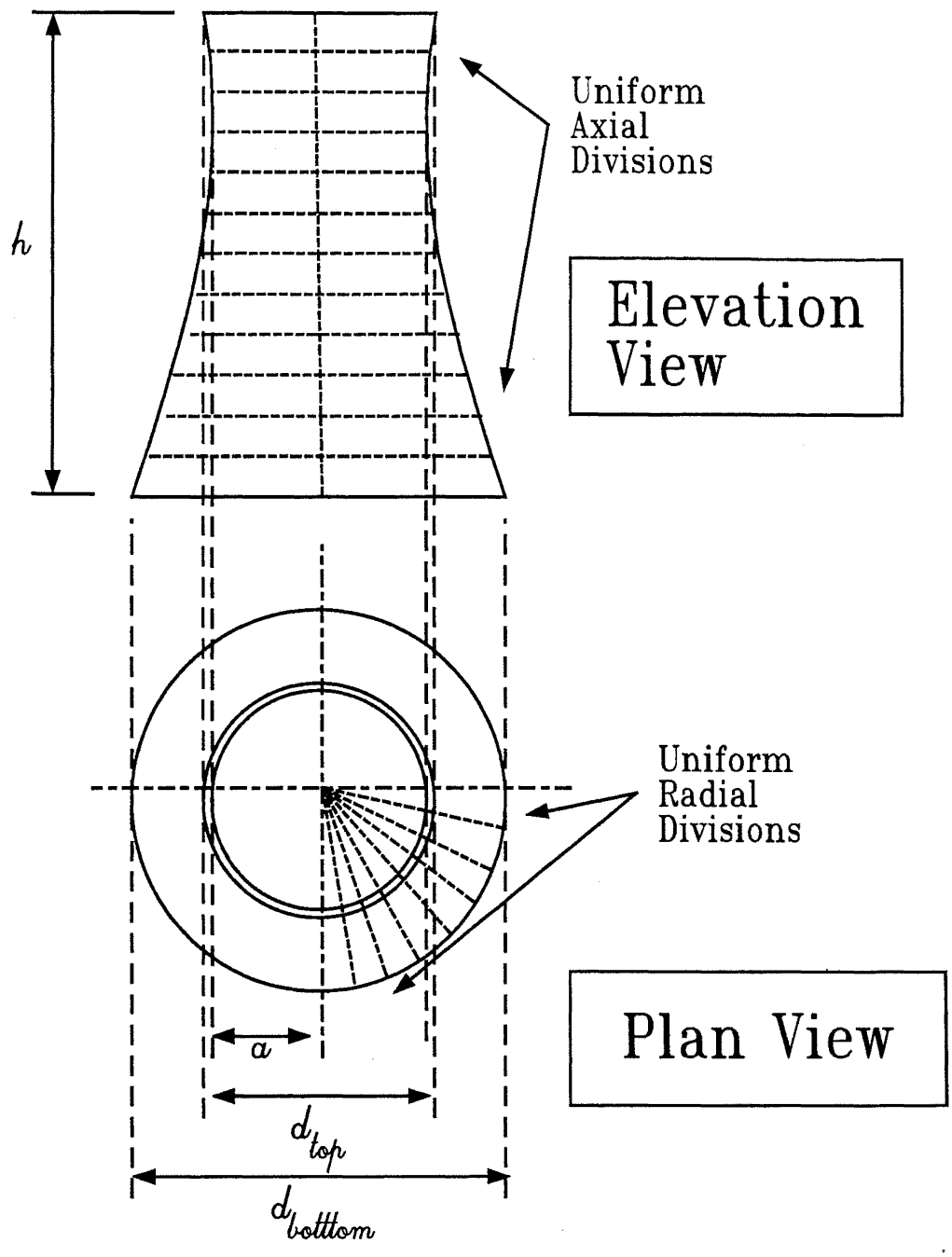

Figure 2-1: Typical Hyperbolic cooling tower and FE Mesh scheme

(Chowdhury, 1990) was developed and used to handle the error calculations. Root mean squared (RMS) value of the error was used to compare errors between different meshes.

$$e^2_{\phi,\,rms} = \frac{1}{n} \sum_{i=1}^{n} e^2_{\phi,\,i}$$

$$e^2_{\theta,\,rms} = \frac{1}{n} \sum_{i=1}^{n} e^2_{\theta,\,i}$$

For comparison between hyperbolic cooling tower shells of different curvature the actual value of the error is normalized by dividing it with RMS value of appropriate shell force over the height. RMS value of the shell forces are calculated from standard solution, using equations similar to the ones for errors.

$$N^2_{\phi,\,rms} = \frac{1}{n} \sum_{i=1}^{n} N^2_{\phi,\,std,\,i}$$

$$N^2_{\theta,\,rms} = \frac{1}{n} \sum_{i=1}^{n} N^2_{\theta,\,std,\,i}$$

$$\bar{e}_{\phi} = \frac{e_{\phi,\,rms}}{N_{\phi,\,rms}} \times 100 \quad (\%)$$

$$\bar{e}_{\theta} = \frac{e_{\theta,\,rms}}{N_{\theta,\,rms}} \times 100 \quad (\%)$$

Chapter 3
Data from FE Analysis

3.1 Overview

This study involved analysis and presentation of large amounts of data. For clarity, the results of FE analysis are presented in graphical form. For each set of FE analysis, actual values of forces (F_ϕ and F_θ), as well as, actual values of errors (e_ϕ and e_θ) are plotted along the height.

Three different hyperbolic cooling tower shells are analyzed using different FE mesh sizes. These structures are similar in all ways except curvature. All three structures have equal height, radius and location of neck and thickness. Only the shell parameter 'b' is varied. It is increased by 20% for a less curved and reduced by 20% for a more curved hyperbolic cooling tower shell.

Structure A : Typical hyperbolic cooling tower shell.

Structure B : Less curved cooling tower.

Structure C : More curved cooling tower.

Results for each of the structures is presented in a different section of this chapter. Along with FE results, corresponding standard solution is also plotted using dotted lines. Maximum numerical value (without sign) and RMS value of errors are found and shown on the figures.

The common data in the analysis of all the shells are given below.

Radius at origin (neck)	$a = 30$ ft.
Coordinate at top of the shell	$z_{top} = 30$ ft.
Coordinate at foot of the shell	$z_{bottom} = -100$ ft.
Shell Thickness	$\delta = 5$ in.
Gravity Loading	$q = 150$ psf
Young's Modulus	$E = 519119.5$ kip/ft^2
Poisson's Ratio	$\nu = 0.15$

3.2 Analysis Results of Structure A

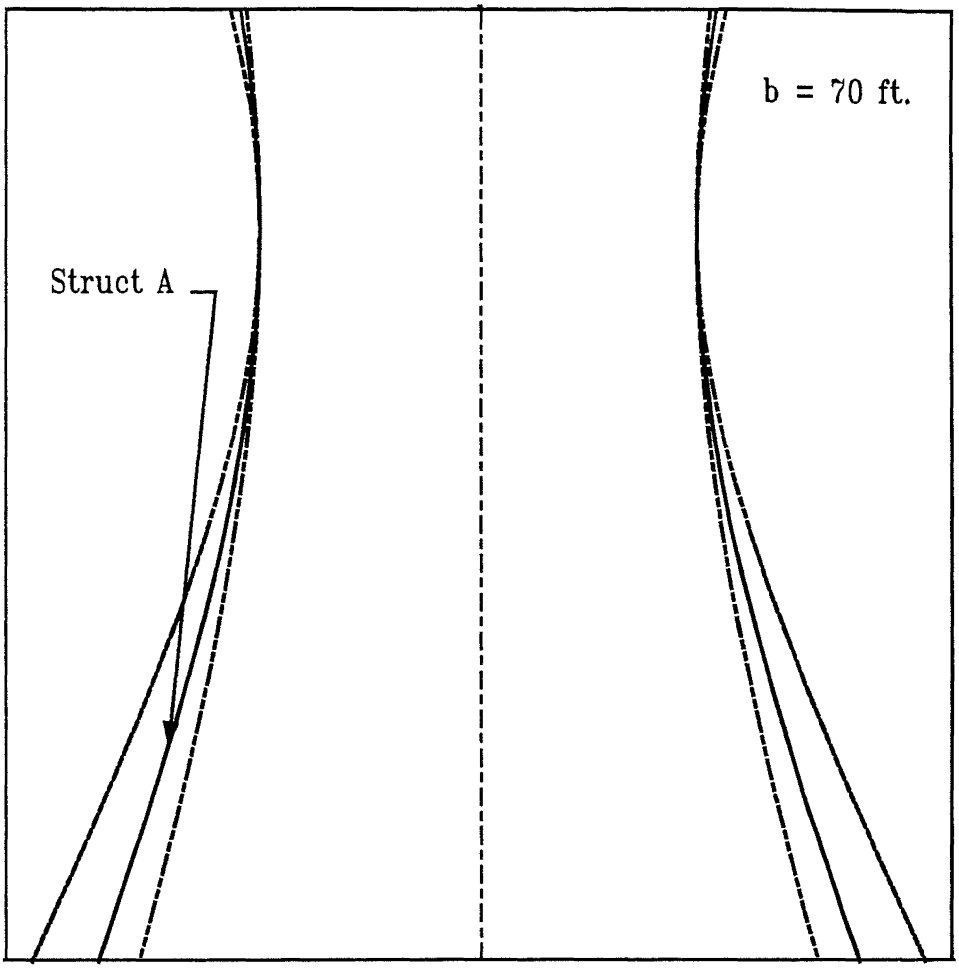

Figure 3-1: Shape of Structure A

RMS value of shell forces for this structure is found (See Sec 2.4) as,

$$N_{\phi,\,rms} = 9.542167 \text{ kip/ft}^2$$

$$N_{\theta,\,rms} = 2.278598 \text{ kip/ft}^2$$

Table 3-1: Summary of Results for Structure A

Mesh Size	$e_{\theta, rms}$ kip/ft	$e_{\phi, rms}$ kip/ft	e_{θ} percent	e_{ϕ} percent	Cost Index
24 * 6	0.550	1.258	24.1	13.2	0.52
24 * 10	0.414	0.752	18.2	7.9	1.60
24 * 12	0.372	0.580	16.3	6.1	2.32
24 * 15	0.330	0.497	14.5	5.2	3.24
12 * 12	0.380	0.614	16.7	6.4	0.46
16 * 12	0.370	0.593	16.2	6.2	0.86
20 * 12	0.370	0.585	16.2	6.1	1.49
24 * 12	0.372	0.580	16.3	6.1	2.32
30 * 12	0.375	0.576	16.5	6.0	3.36

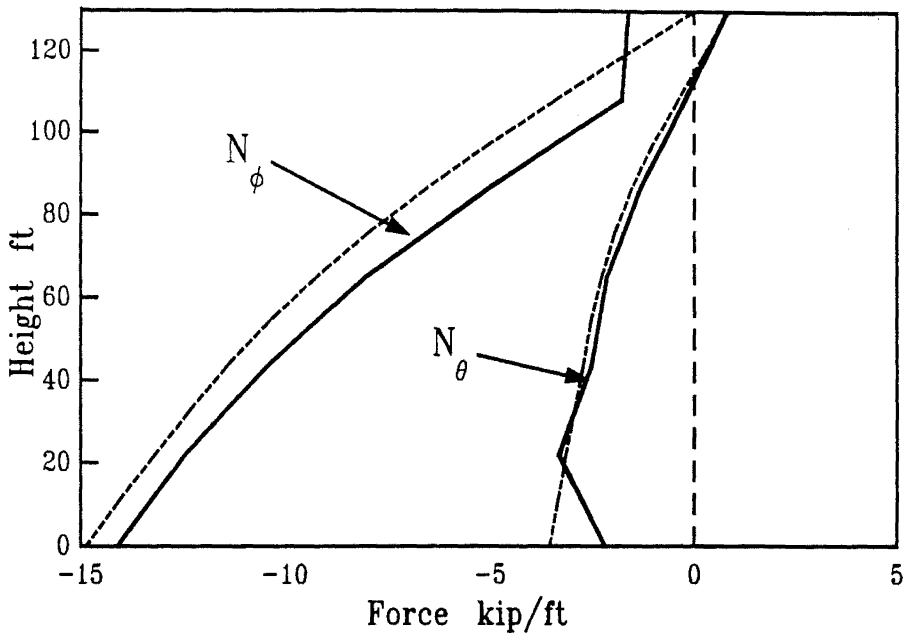

Fig. A

Shell Forces Along Height

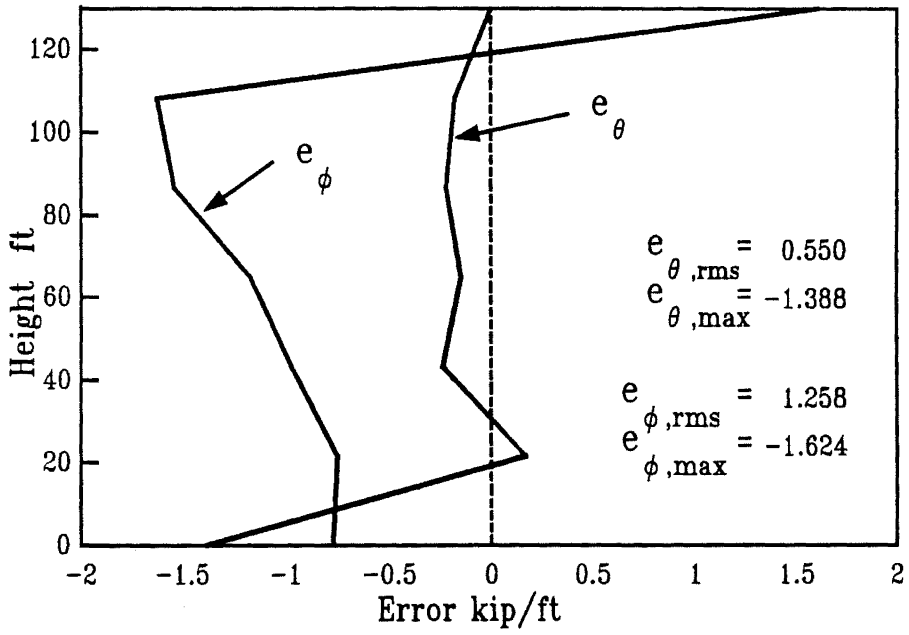

Fig. B

Error Distribution Along Height

Figure 3-2: Results for Structure A : Mesh size 24 * 6

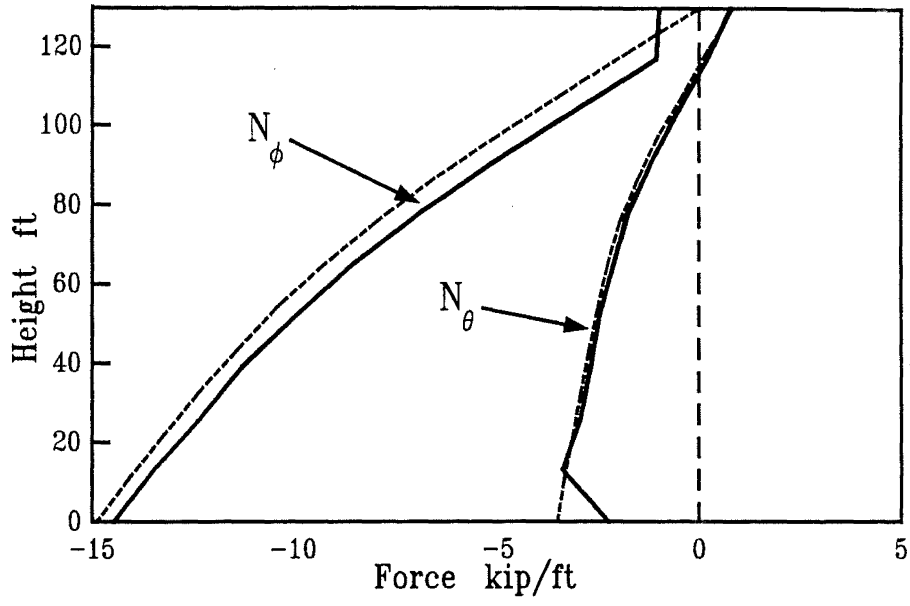

Fig. A

Shell Forces Along Height

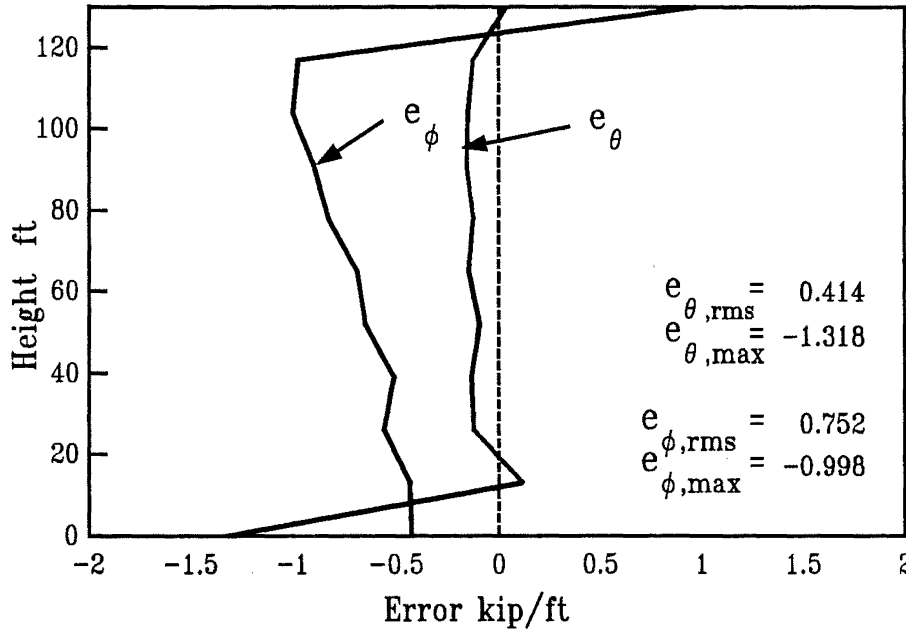

Fig. B

Error Distribution Along Height

Figure 3-3: Results for Structure A : Mesh size 24 * 10

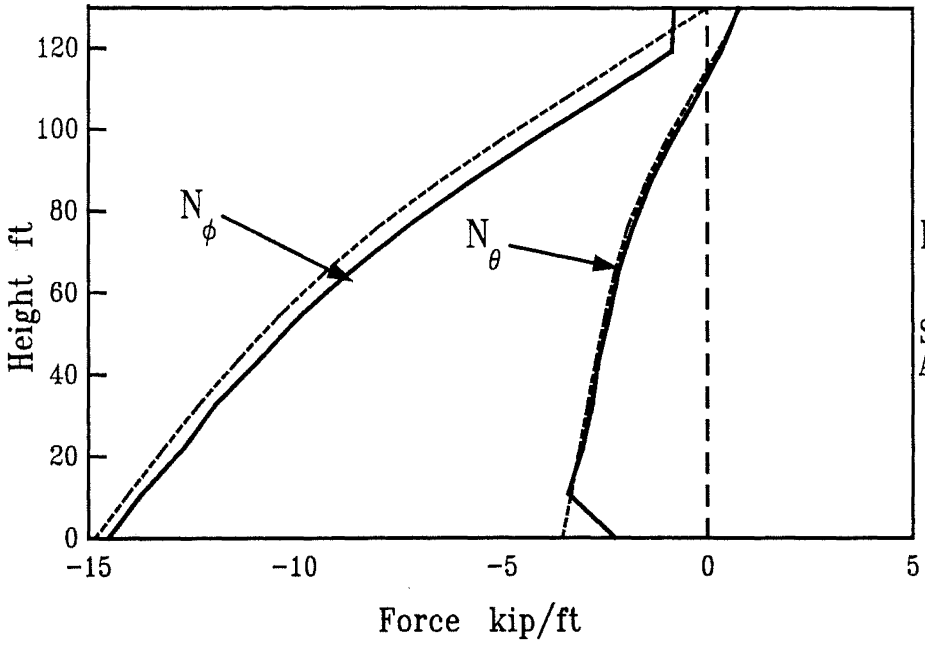

Fig. A

Shell Forces Along Height

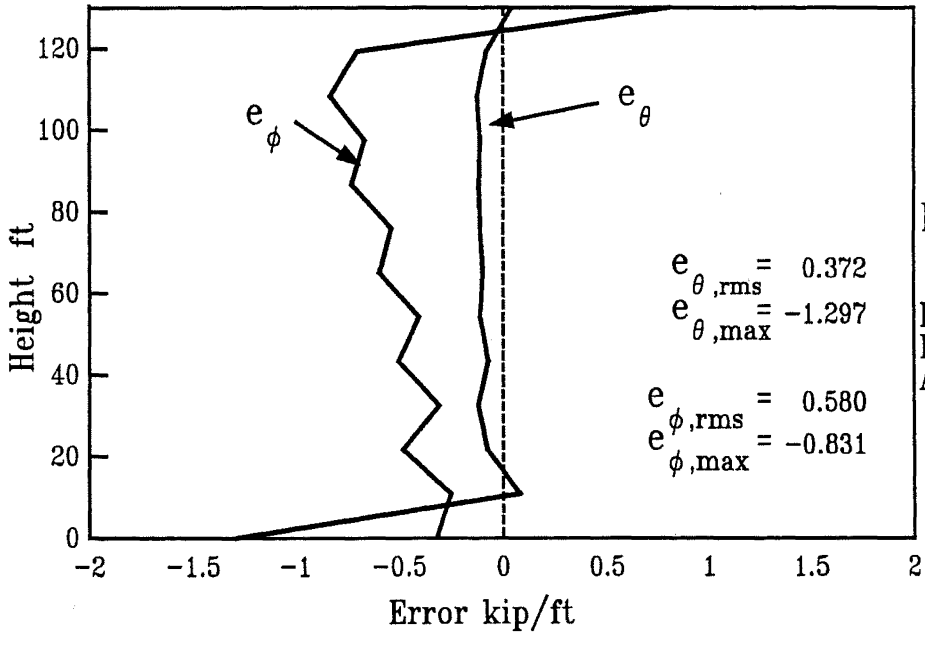

Fig. B

Error Distribution Along Height

Figure 3-4: Results for Structure A : Mesh size 24 * 12

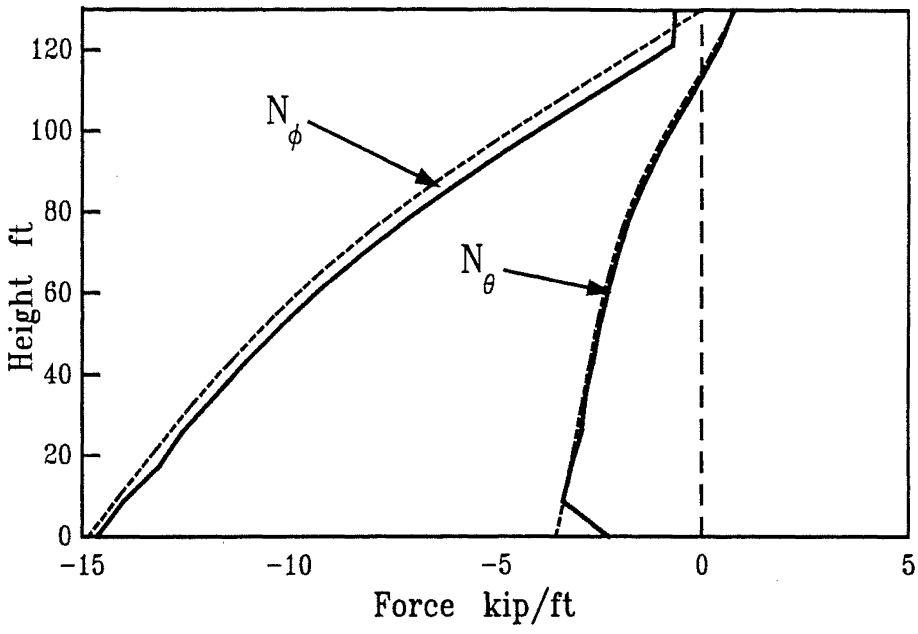

Fig. A

Shell Forces Along Height

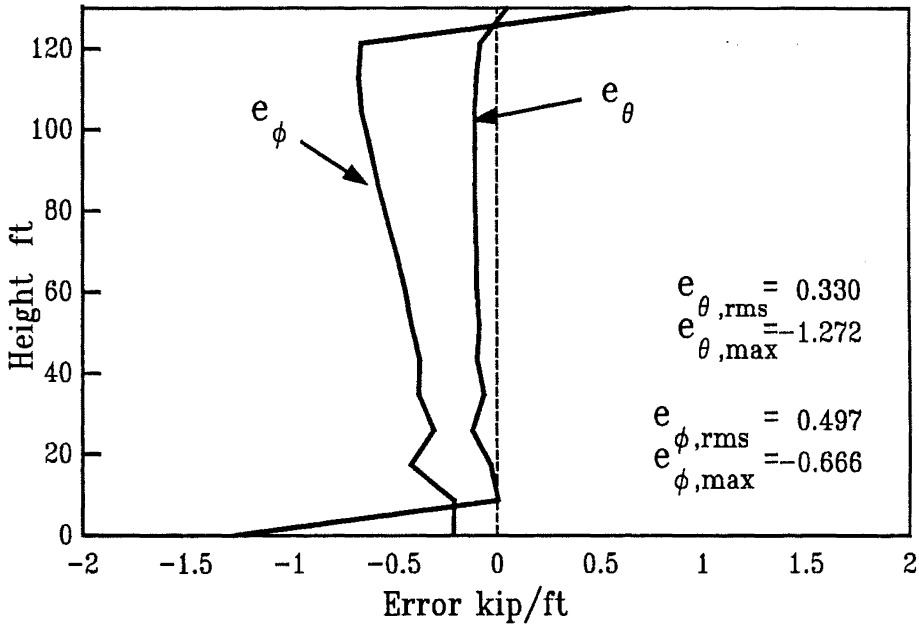

Fig. B

Error Distribution Along Height

Figure 3-5: Results for Structure A : Mesh size 24 * 15

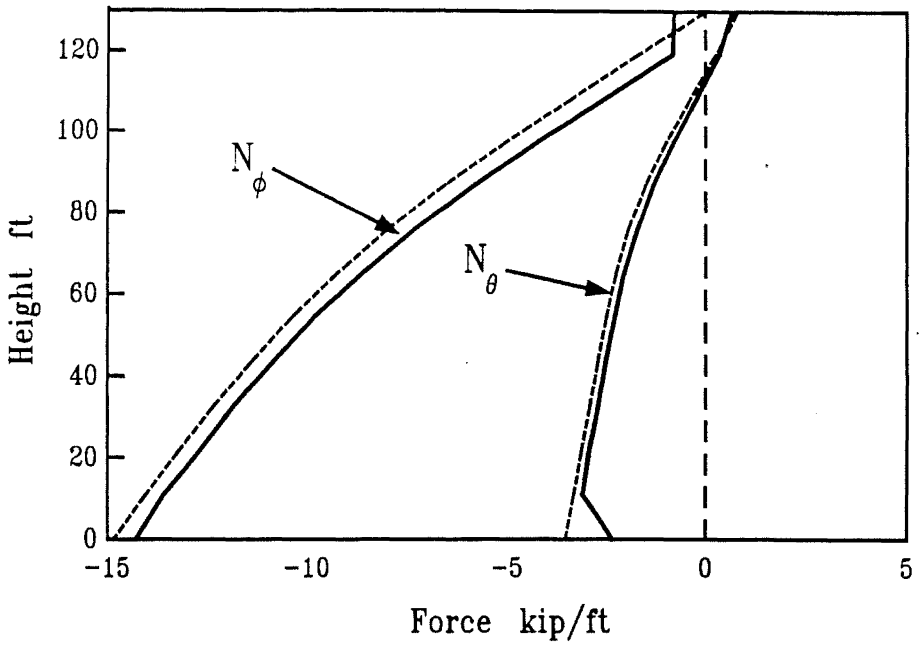

Fig. A

Shell Forces Along Height

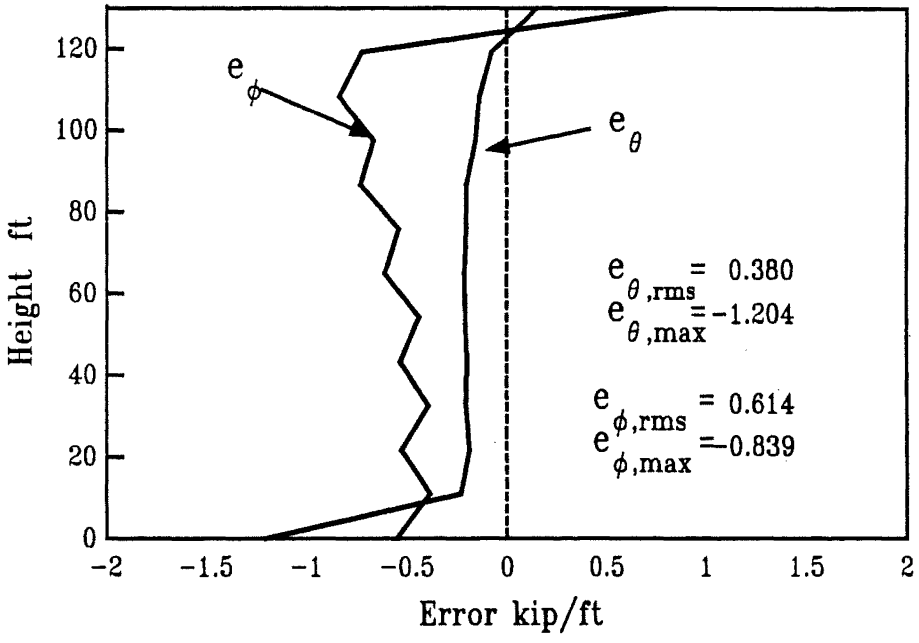

Fig. B

Error Distribution Along Height

Figure 3-6: Results for Structure A : Mesh size 12 * 12

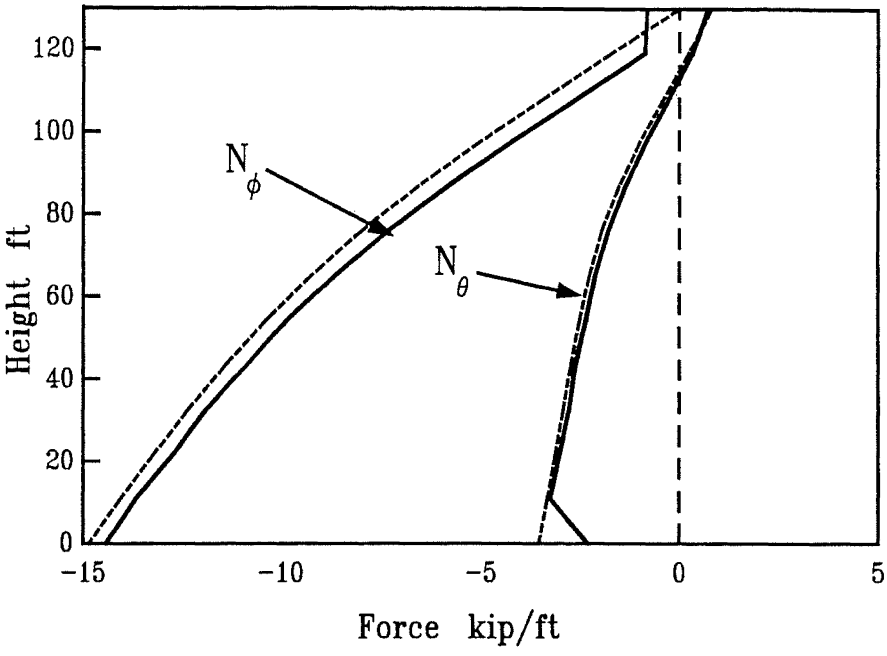

Fig. A

Shell Forces Along Height

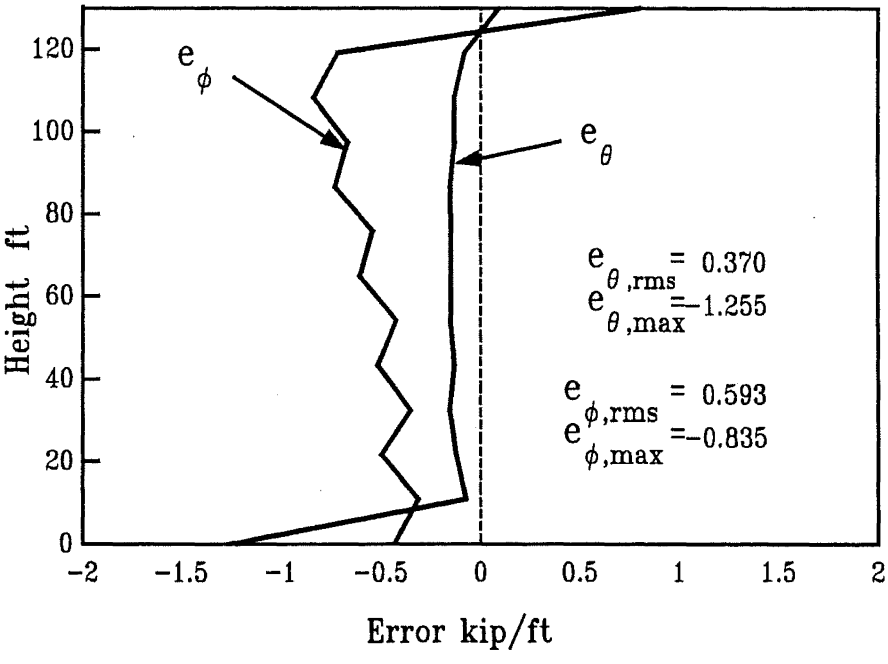

Fig. B

Error Distribution Along Height

Figure 3-7: Results for Structure A : Mesh size 16 * 12

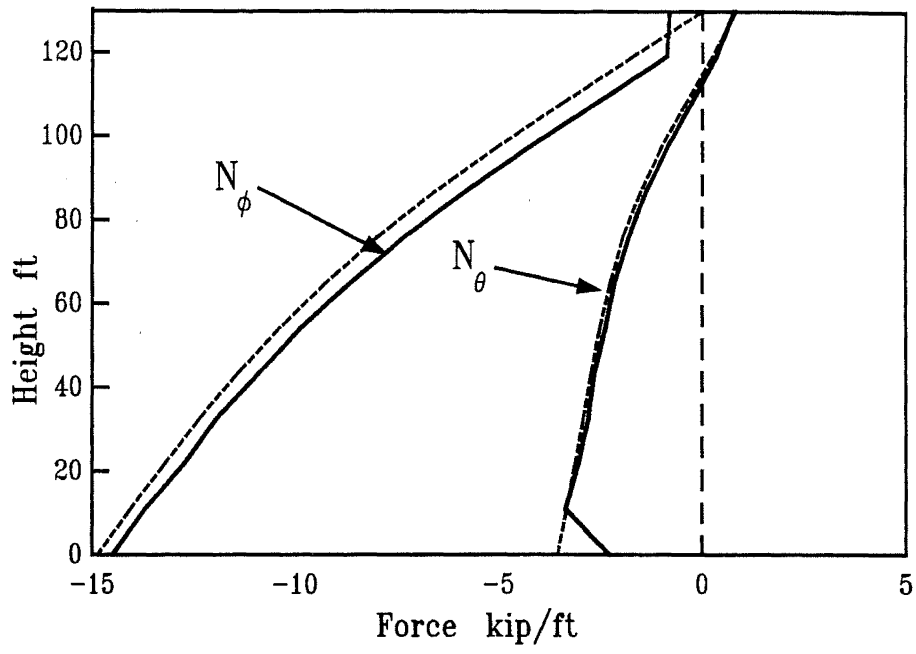

Fig. A

Shell Forces Along Height

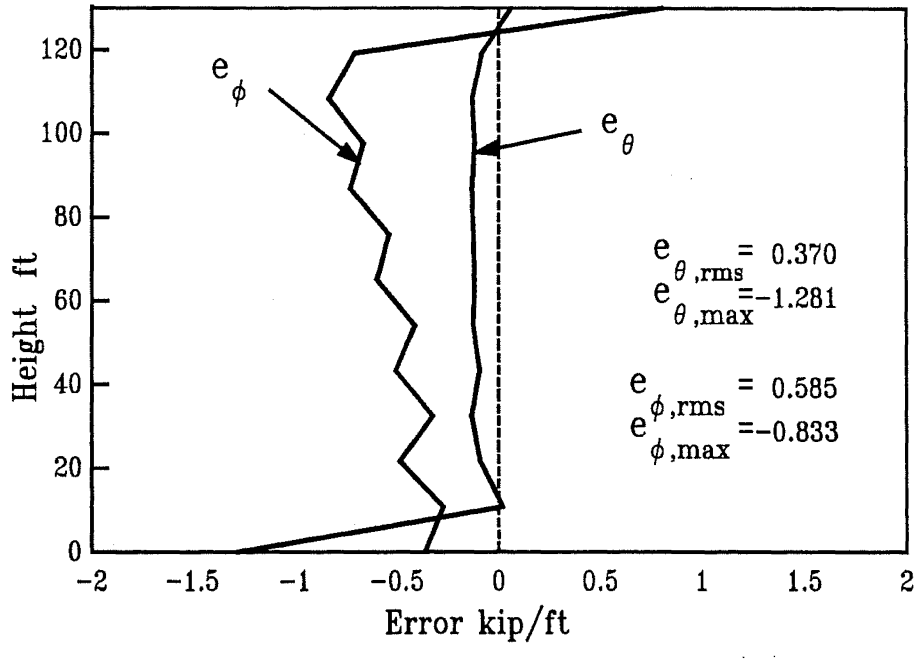

Fig. B

Error Distribution Along Height

Figure 3-8: Results for Structure A : Mesh size 20 * 12

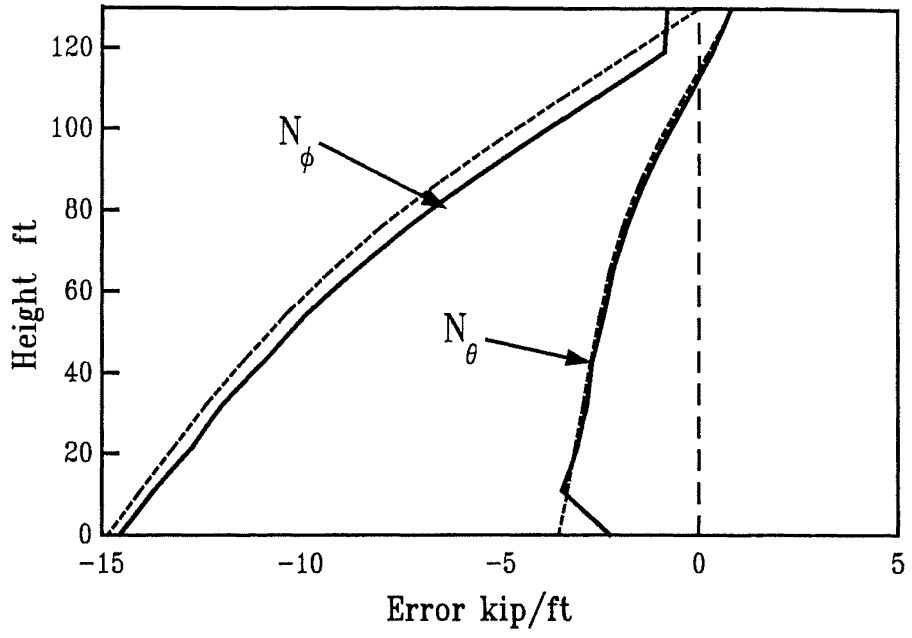

Fig. A

Shell Forces Along Height

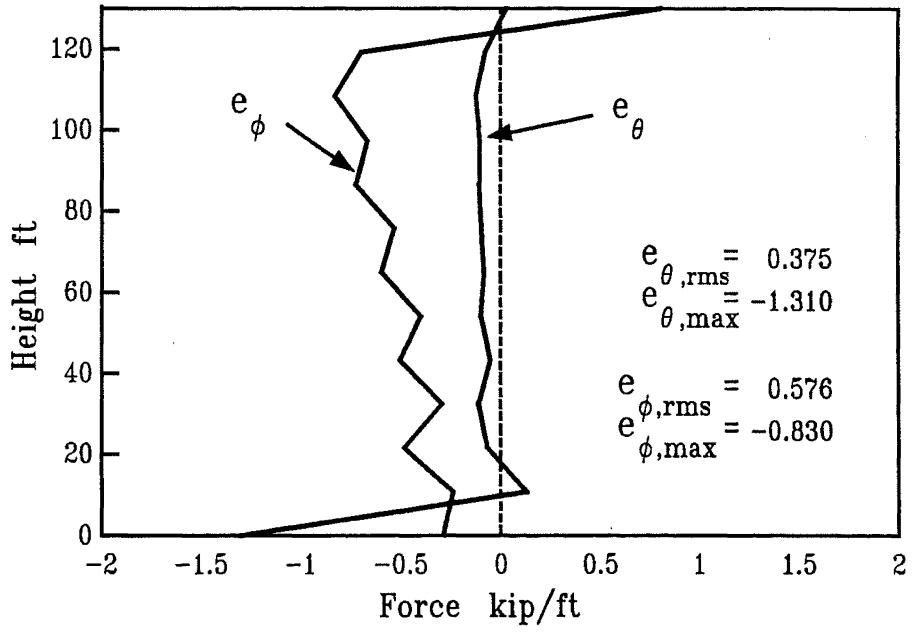

Fig. B

Error Distribution Along Height

Figure 3-9: Results for Structure A : Mesh size 30 * 12

3.3 Analysis Results of Structure B

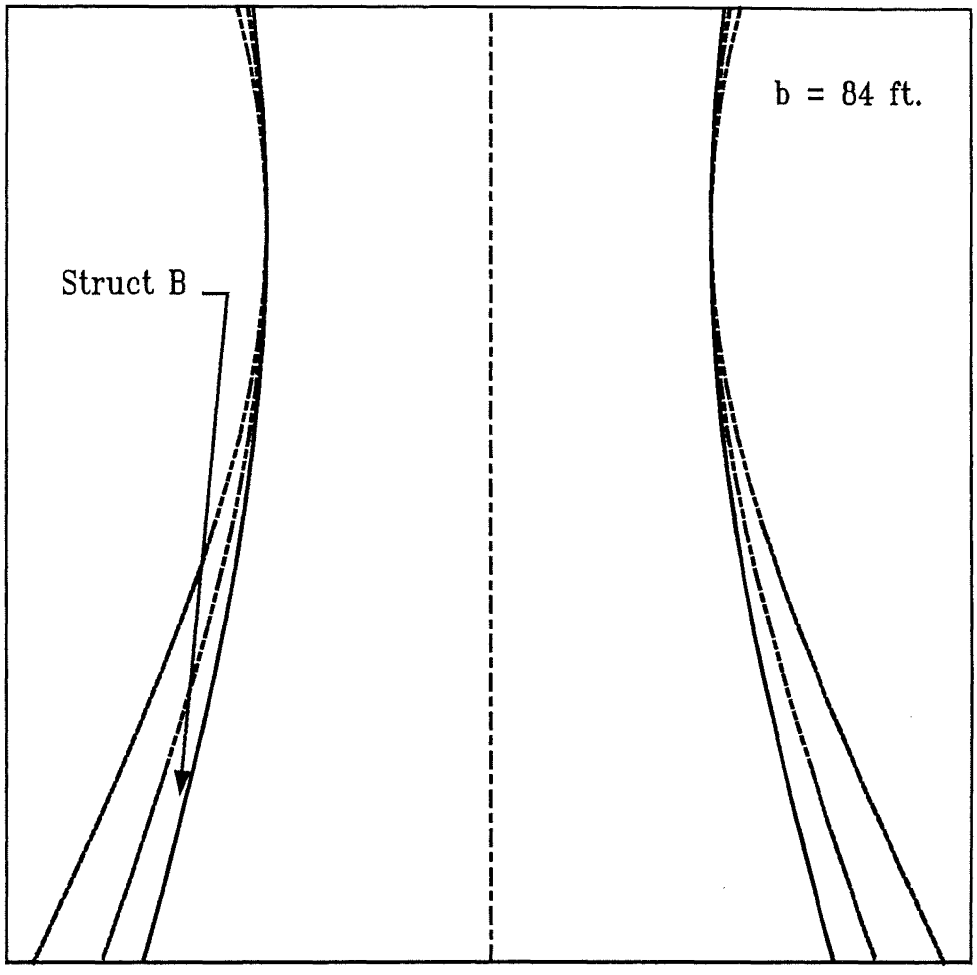

Figure 3-10: Shape of Structure B

RMS value of shell forces for this structure is found (See Sec 2.4) as,

$$N_{\phi,\,rms} = 9.751214\ \text{kip/ft}^2$$

$$N_{\theta,\,rms} = 1.700731\ \text{kip/ft}^2$$

Table 3-2: Summary of Results for Structure B

Mesh Size	$e_{\theta,\ rms}$ kip/ft	$e_{\phi,\ rms}$ kip/ft	e_{θ} percent	e_{ϕ} percent	Cost Index
24 * 6	0.234	1.302	13.8	13.4	0.52
24 * 10	0.168	0.780	9.9	8.0	1.54
24 * 12	0.145	0.604	8.5	6.2	2.24
24 * 15	0.128	0.518	7.5	5.3	3.22
12 * 12	0.187	0.623	11.0	6.4	0.47
16 * 12	0.160	0.612	9.4	6.3	0.86
20 * 12	0.150	0.607	8.8	6.2	1.50
24 * 12	0.145	0.604	8.5	6.2	2.24
30 * 12	0.142	0.602	8.3	6.2	3.39

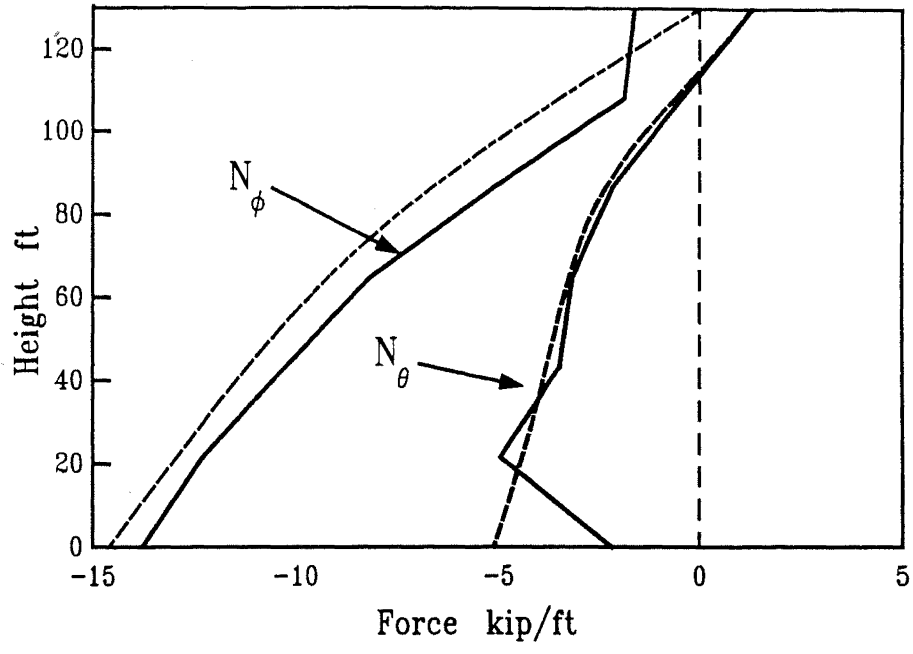

Fig. A

Shell Forces Along Height

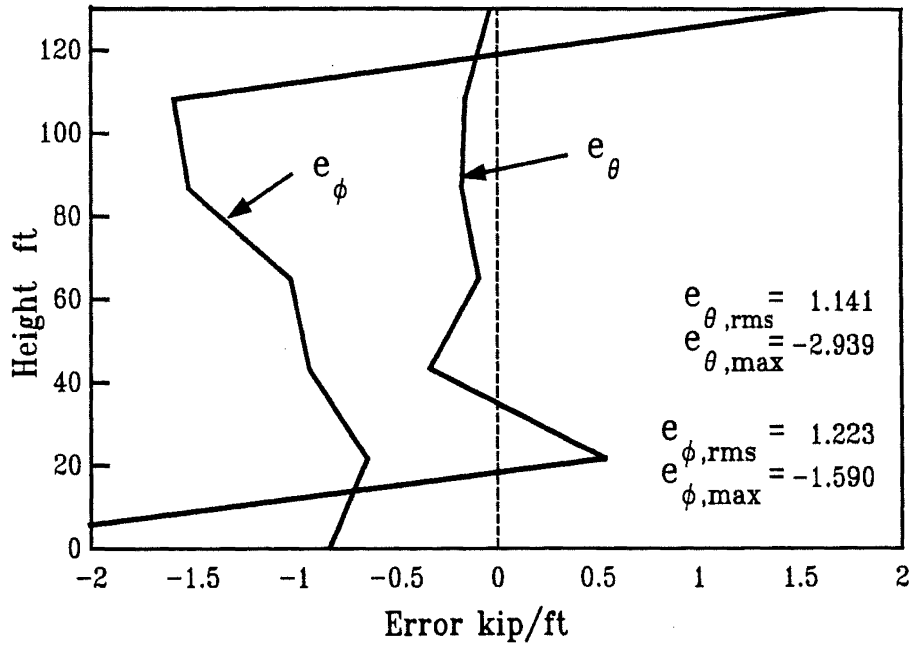

Fig. B

Error Distribution Along Height

Figure 3-11: Results for Structure B : Mesh size 24 * 6

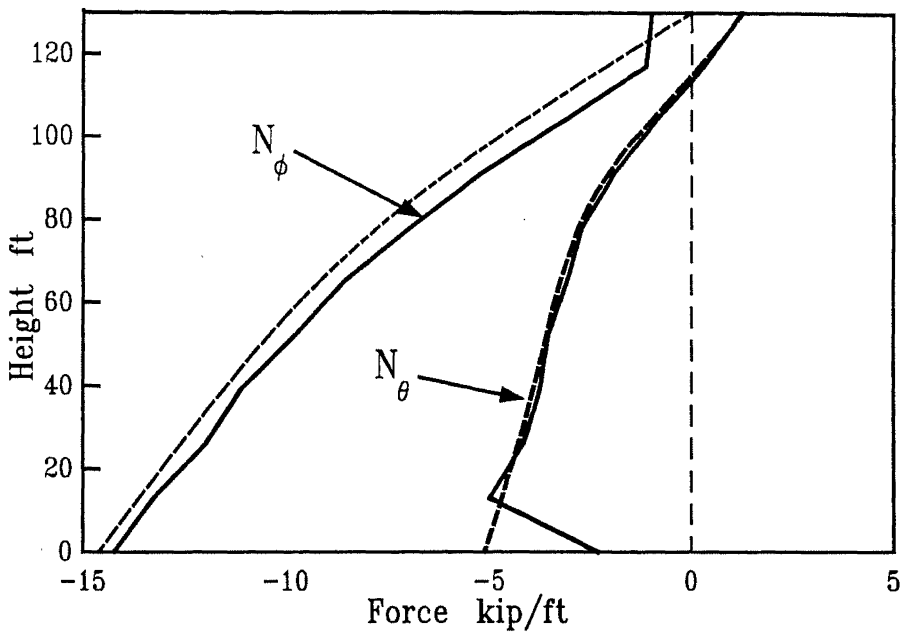

Fig. A

Shell Forces Along Height

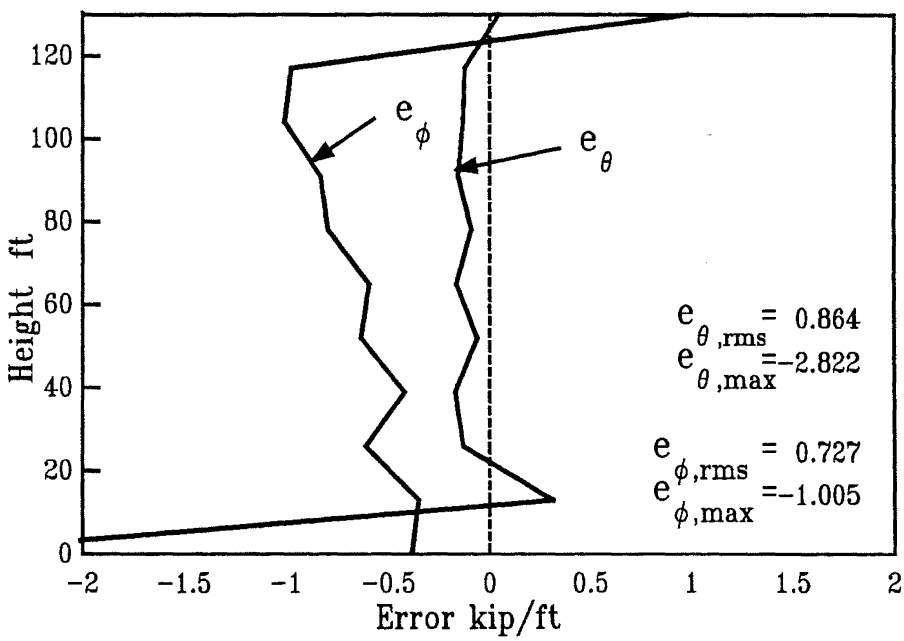

Fig. B

Error Distribution Along Height

Figure 3-12: Results for Structure B : Mesh size 24 * 10

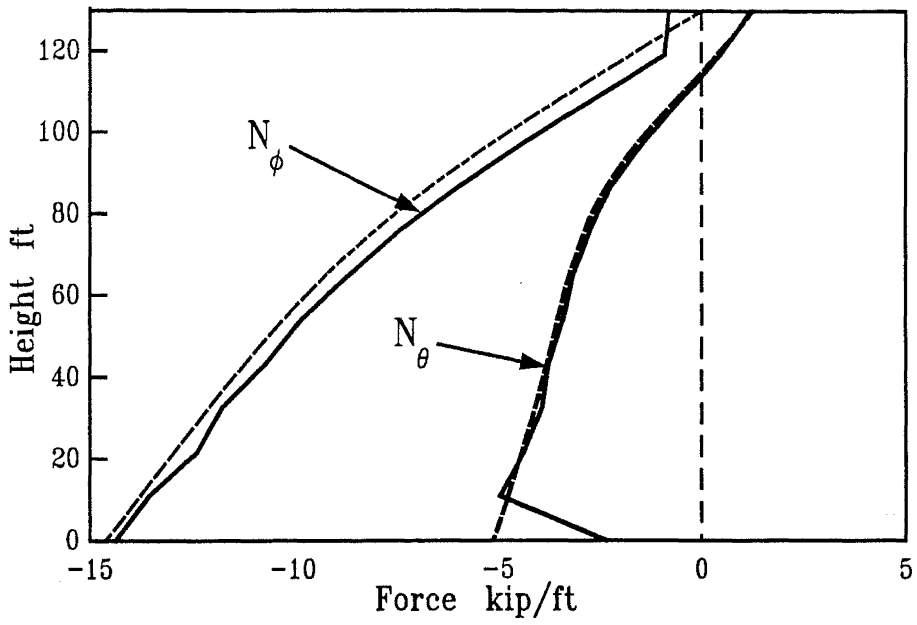

Fig. A

Shell Forces Along Height

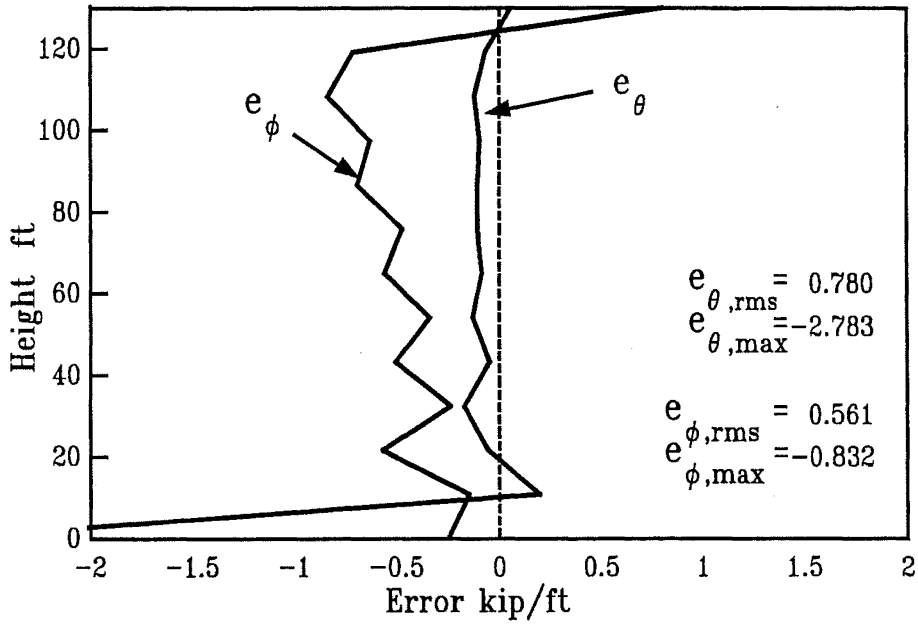

Fig. B

Error Distribution Along Height

Figure 3-13: Results for Structure B : Mesh size 24 * 12

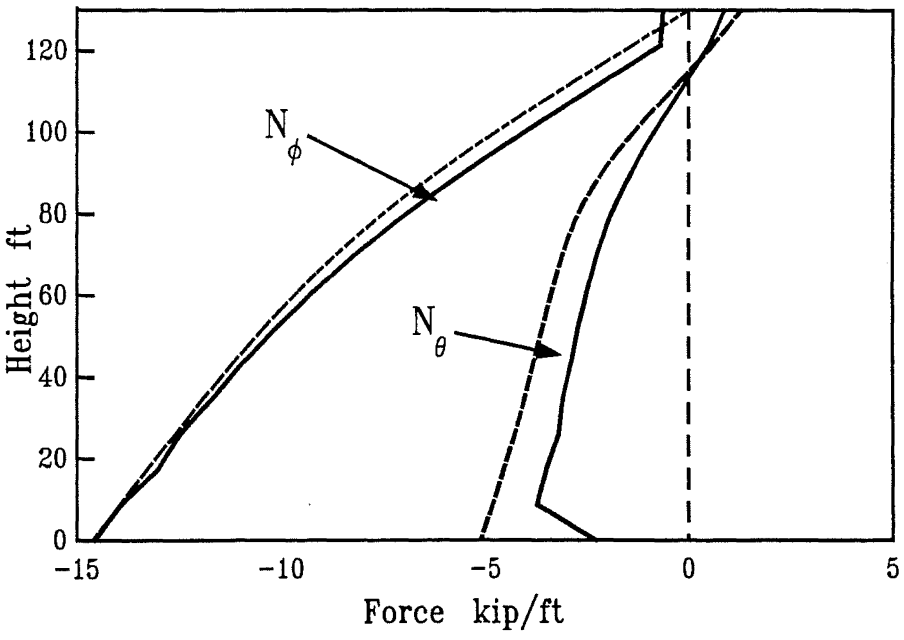

Fig. A

Shell Forces Along Height

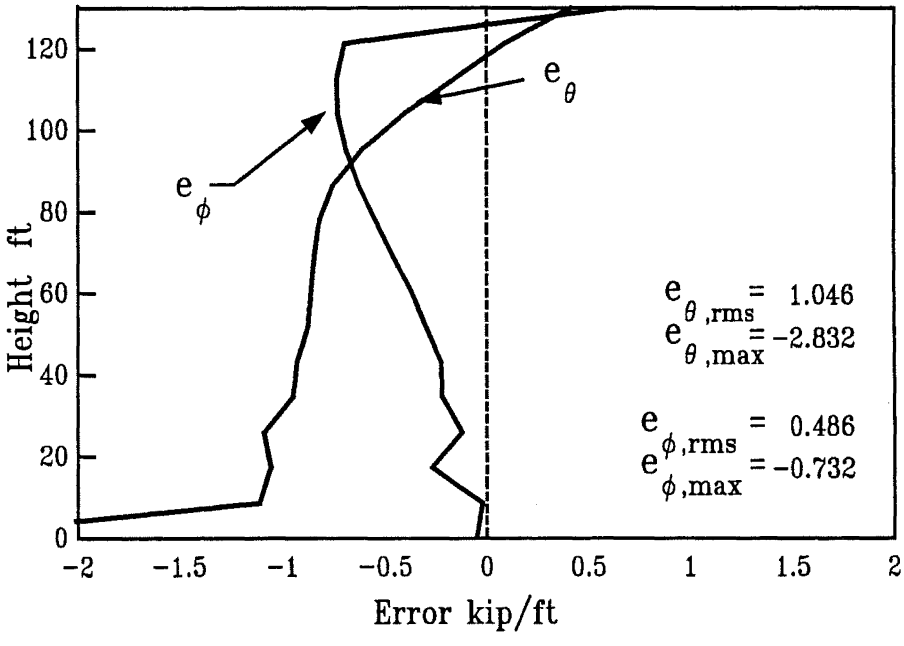

Fig. B

Error Distribution Along Height

Figure 3-14: Results for Structure B : Mesh size 24 * 15

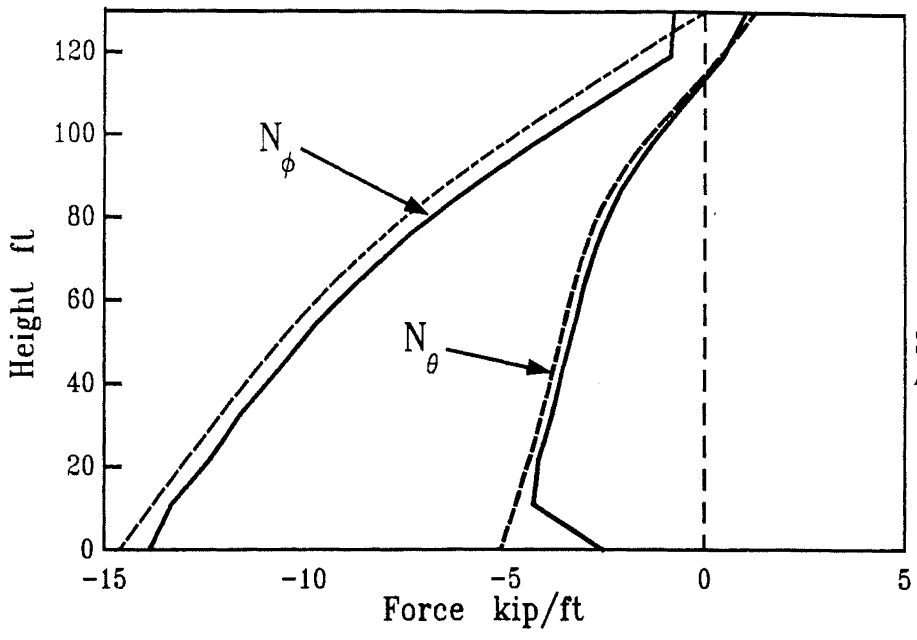

Fig. A

Shell Forces Along Height

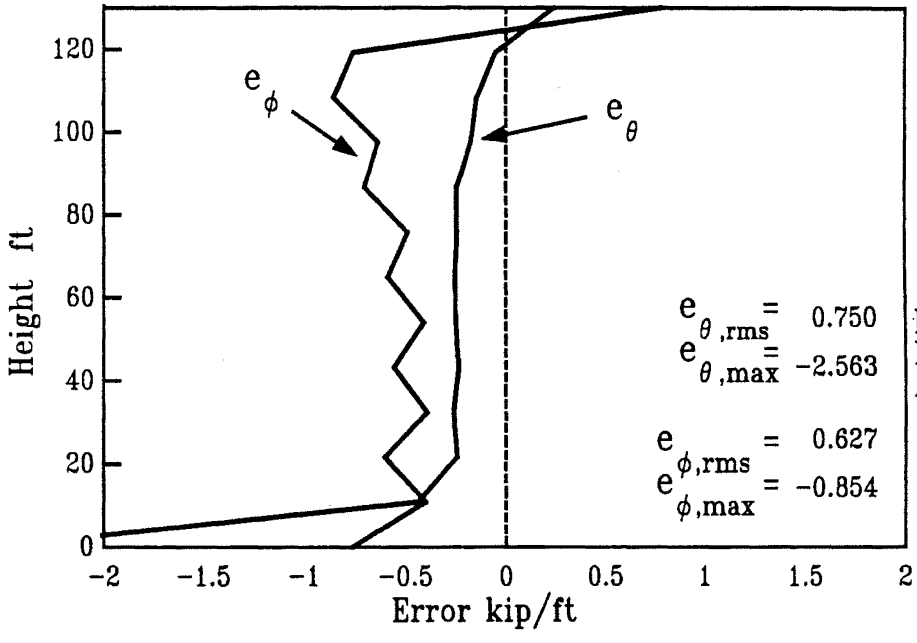

Fig. B

Error Distribution Along Height

Figure 3-15: Results for Structure B : Mesh size 12 * 12

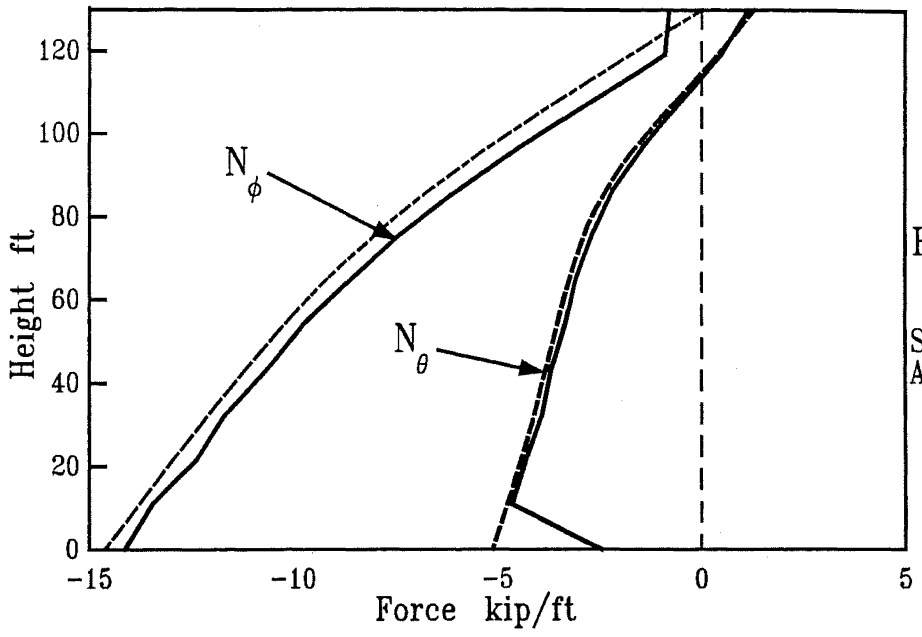

Fig. A

Shell Forces Along Height

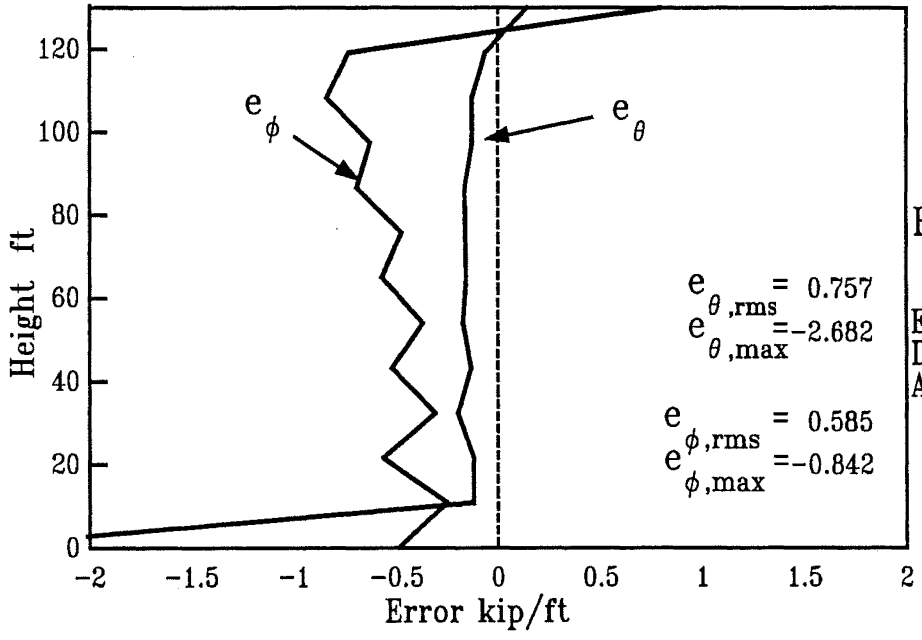

Fig. B

Error Distribution Along Height

Figure 3-16: Results for Structure B : Mesh size 16 * 12

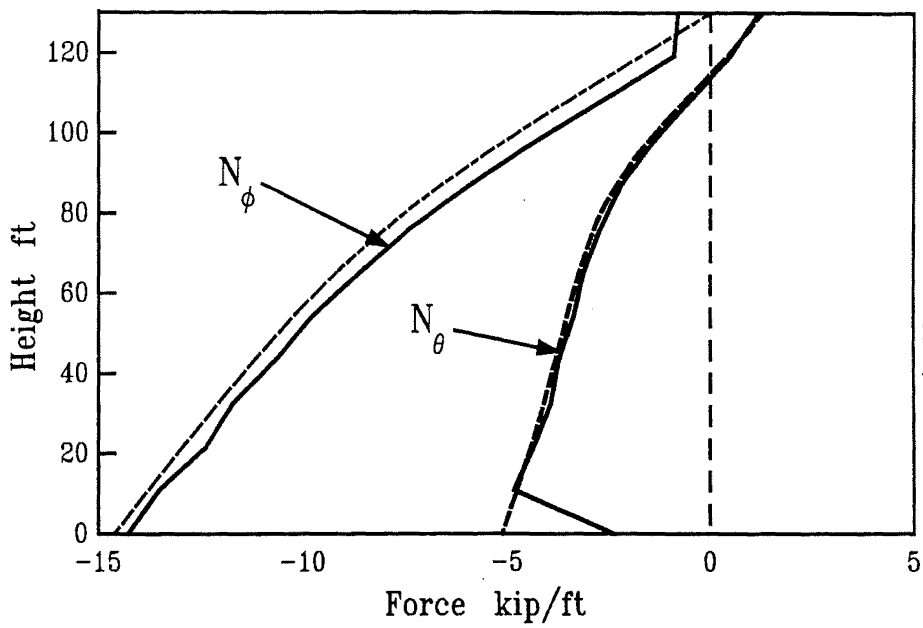

Fig. A

Shell Forces Along Height

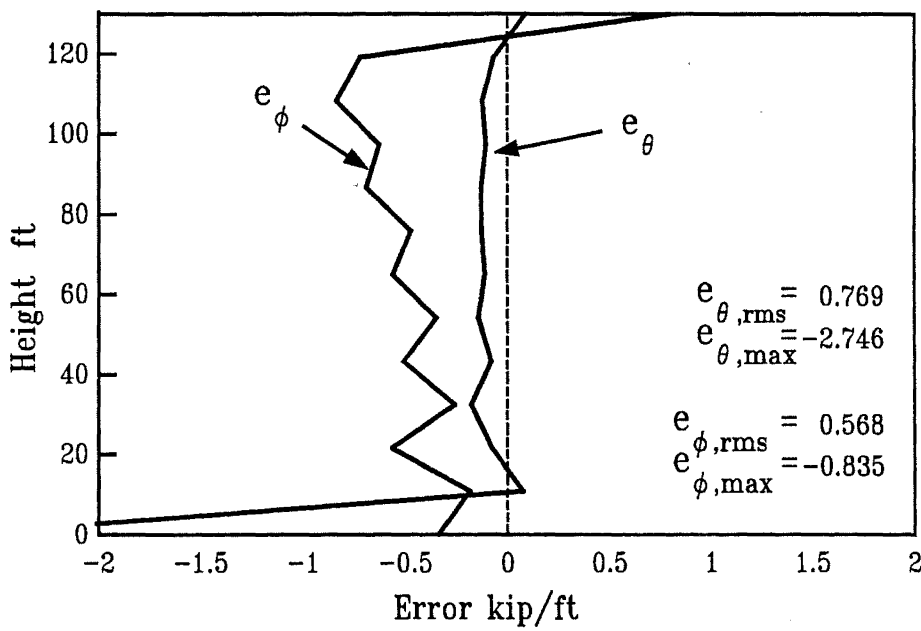

Fig. B

Error Distribution Along Height

Figure 3-17: Results for Structure B : Mesh size 20 * 12

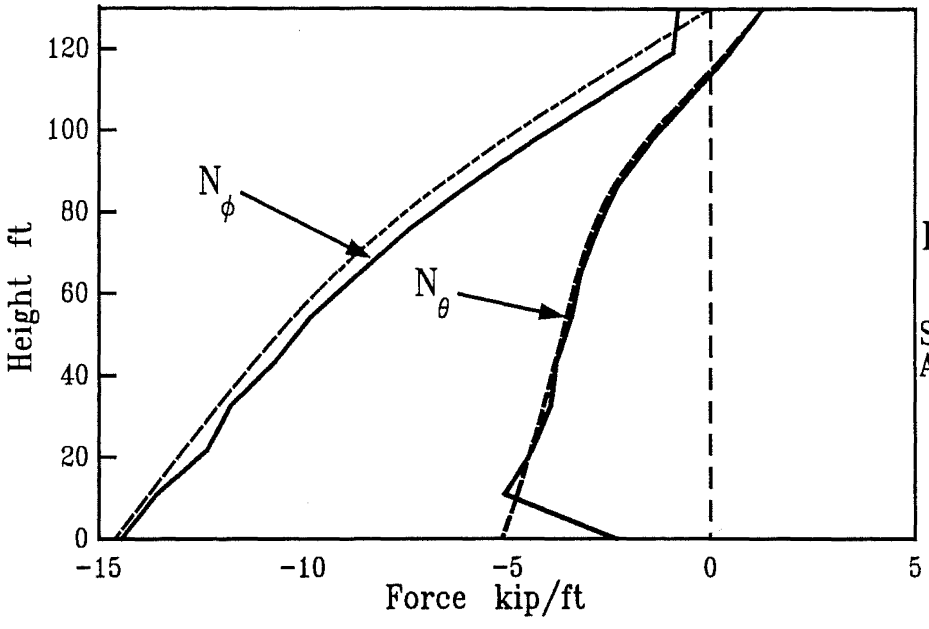

Fig. A

Shell Forces Along Height

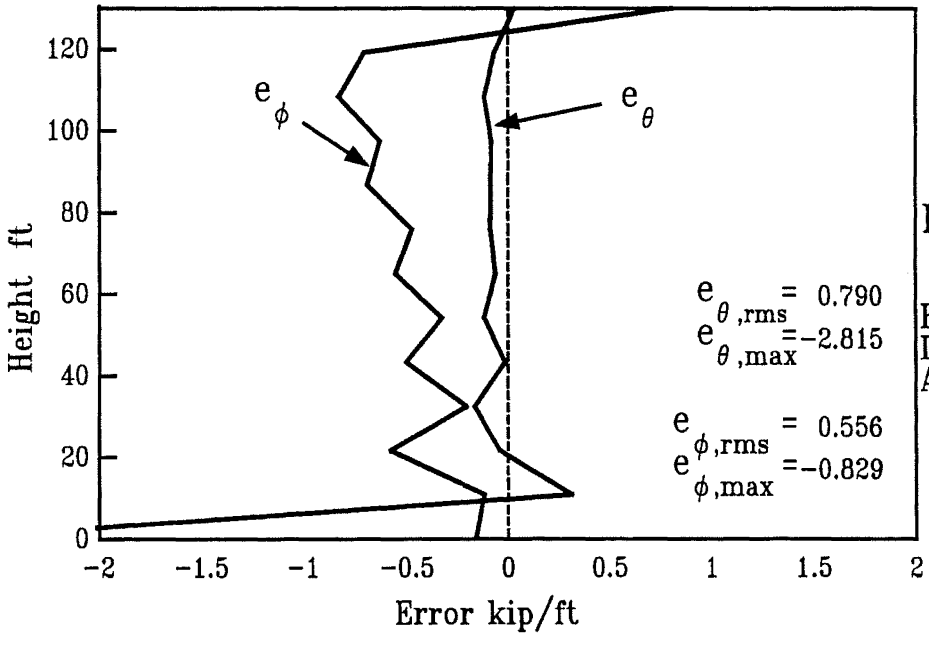

Fig. B

Error Distribution Along Height

Figure 3-18: Results for Structure B : Mesh size 30 * 12

3.4 Analysis Results of Structure C

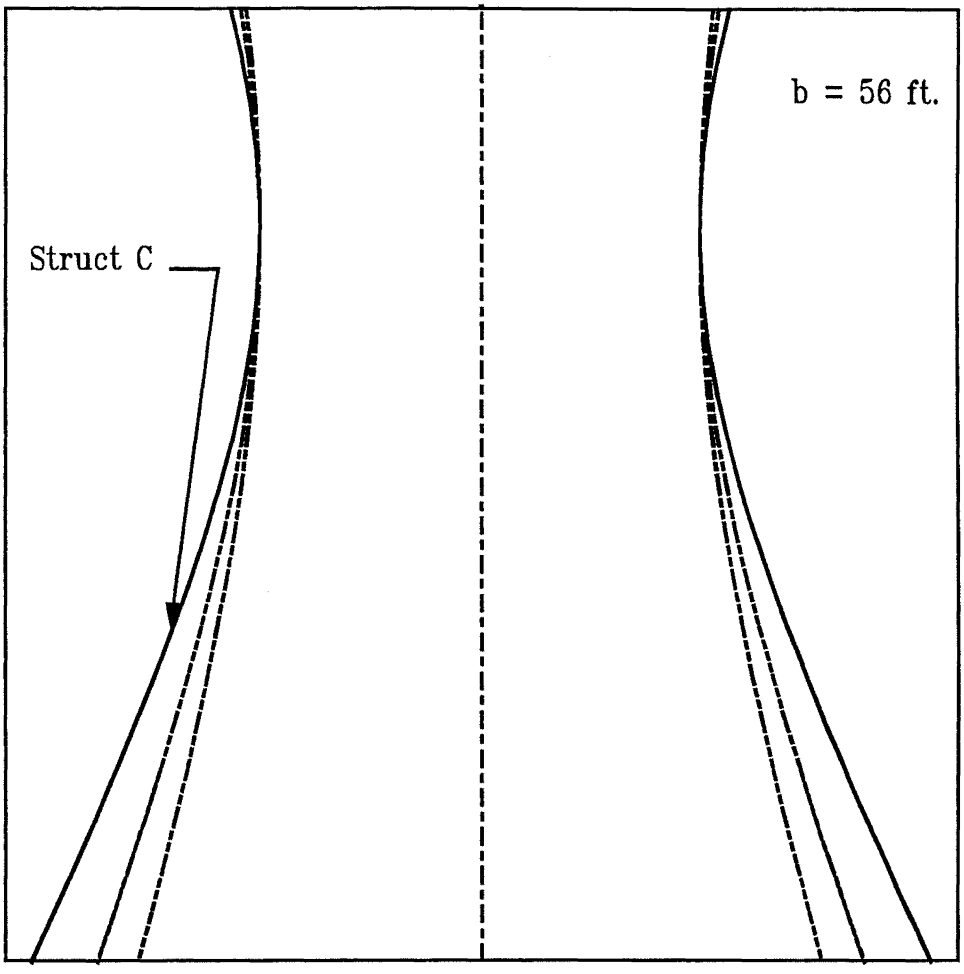

Figure 3-19: Shape of Structure C

RMS value of shell forces for this structure is found (See Sec 2.4) as,

$$N_{\phi,\,rms} = 9.412002 \text{ kip/ft}^2$$

$$N_{\theta,\,rms} = 3.256484 \text{ kip/ft}^2$$

Table 3-3: Summary of Results for Structure C

Mesh Size	$e_{\theta, rms}$ kip/ft	$e_{\phi, rms}$ kip/ft	e_{θ} percent	e_{ϕ} percent	Cost Index
24 * 6	1.141	1.223	35.0	13.0	0.52
24 * 10	0.864	0.727	26.5	7.7	1.57
24 * 12	0.780	0.561	24.0	6.0	2.27
24 * 15	1.046	0.486	32.1	5.2	3.27
12 * 12	0.750	0.627	23.0	6.7	0.48
16 * 12	0.757	0.585	23.2	6.2	0.86
20 * 12	0.769	0.568	23.6	6.0	1.51
24 * 12	0.780	0.561	24.0	6.0	2.27
30 * 12	0.790	0.556	24.3	5.9	3.43

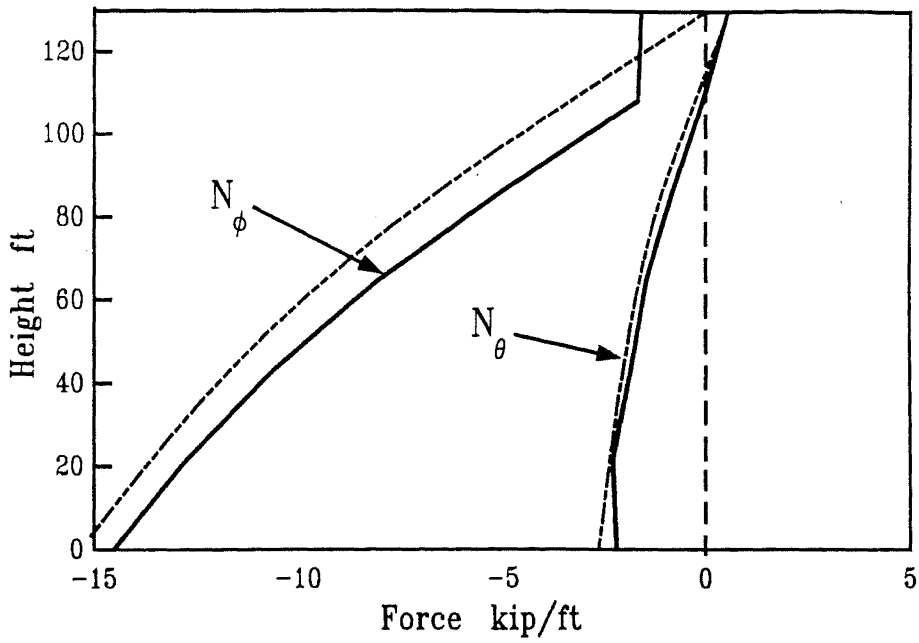

Fig. A

Shell Forces Along Height

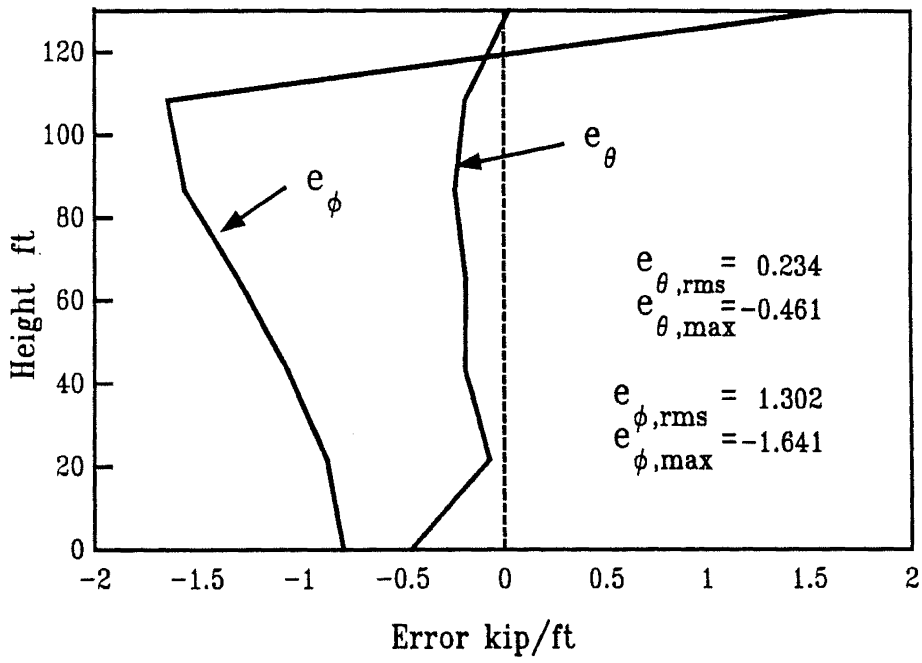

Fig. B

Error Distribution Along Height

Figure 3-20: Results for Structure C : Mesh size 24 * 6

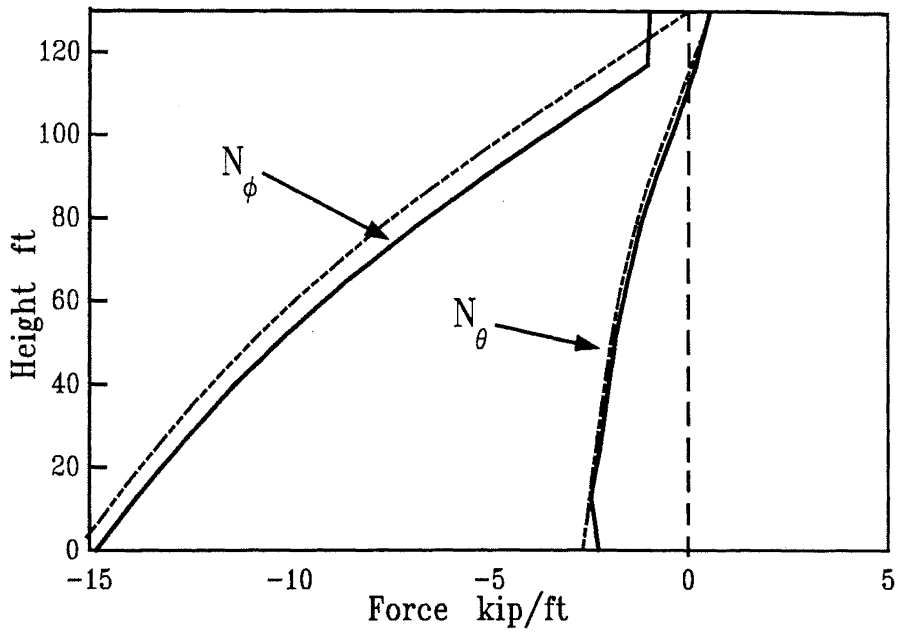

Fig. A

Shell Forces Along Height

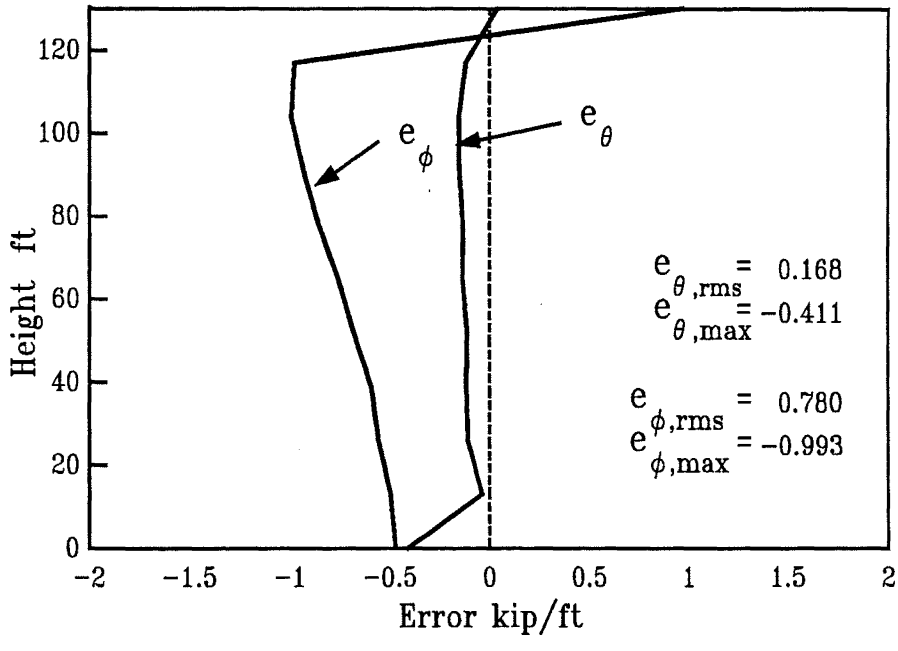

Fig. B

Error Distribution Along Height

Figure 3-21: Results for Structure C : Mesh size 24 * 10

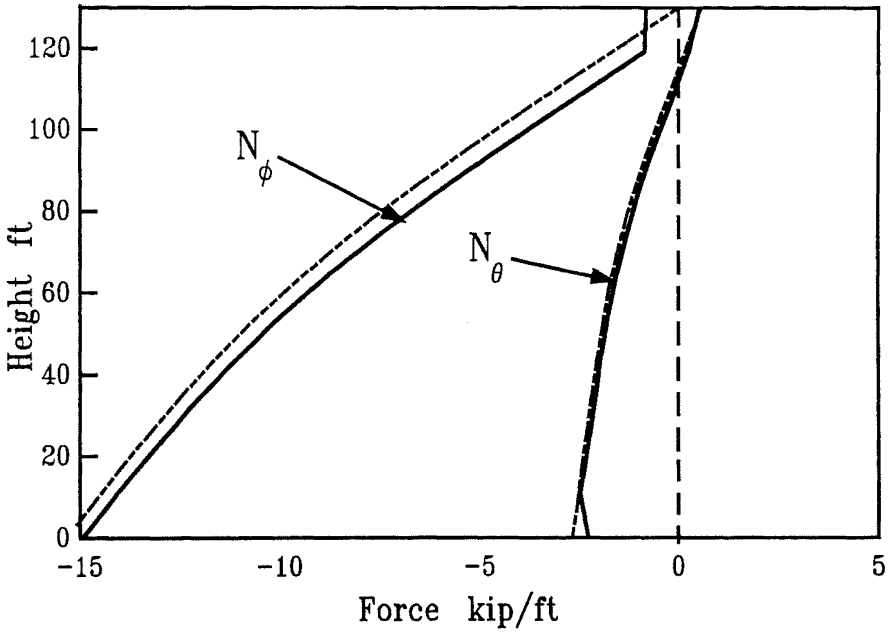

Fig. A

Shell Forces Along Height

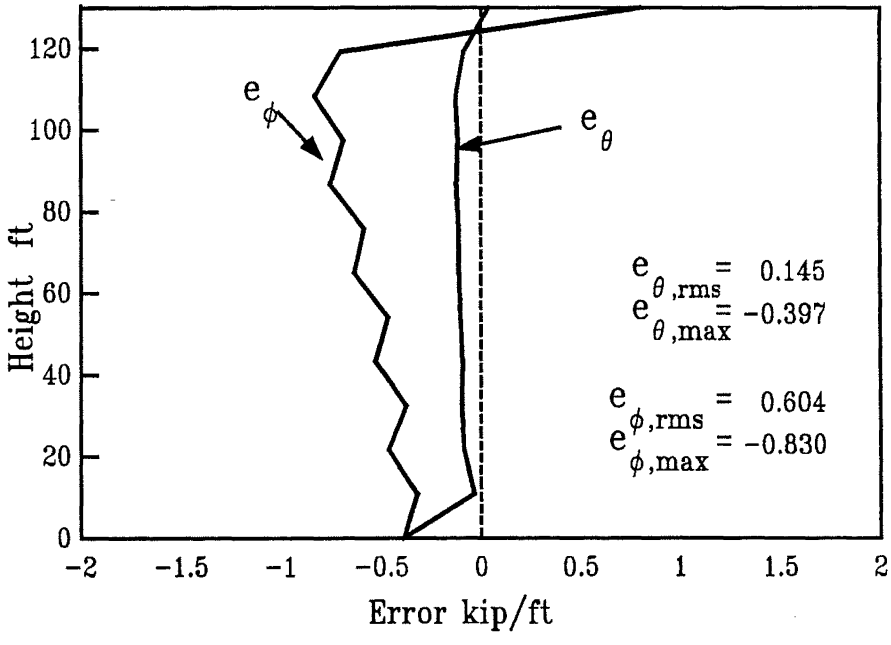

Fig. B

Error Distribution Along Height

Figure 3-22: Results for Structure C : Mesh size 24 * 12

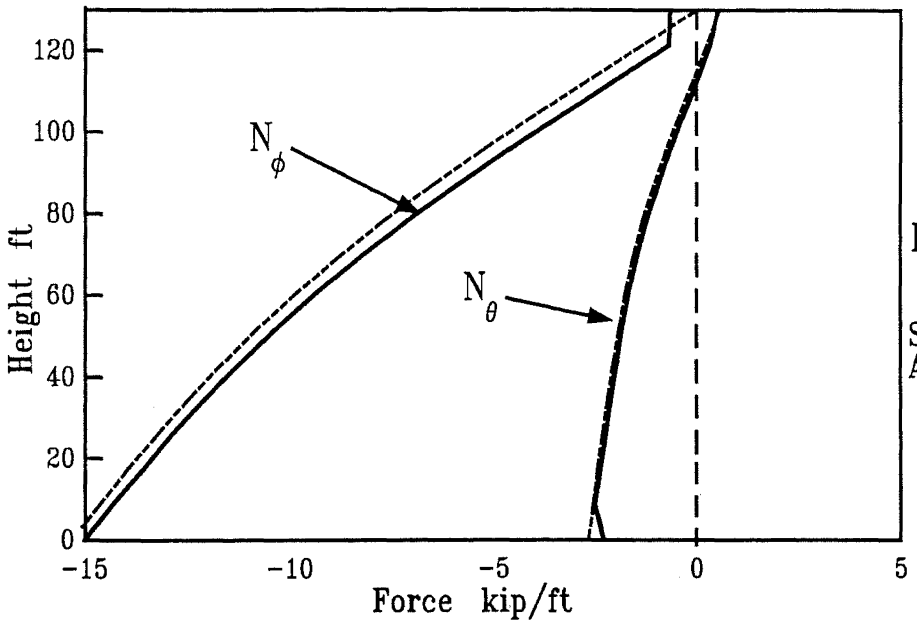

Fig. A

Shell Forces Along Height

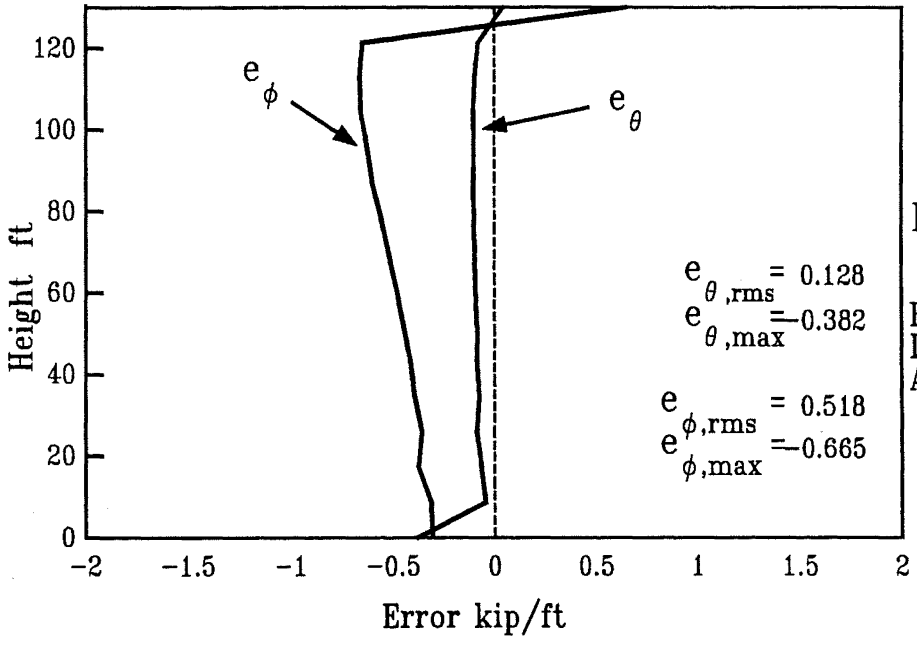

Fig. B

Error Distribution Along Height

Figure 3-23: Results for Structure C : Mesh size 24 * 15

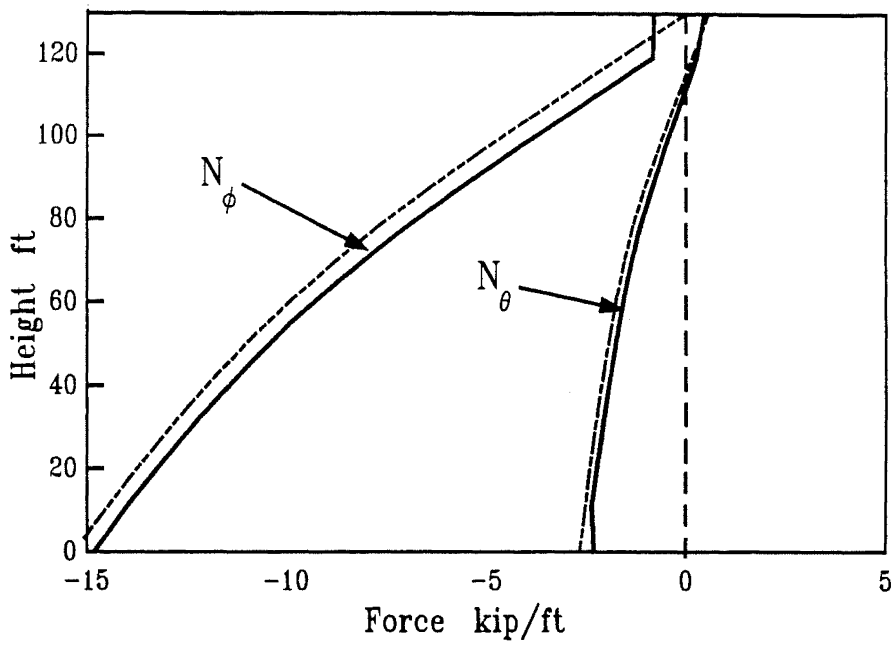

Fig. A

Shell Forces Along Height

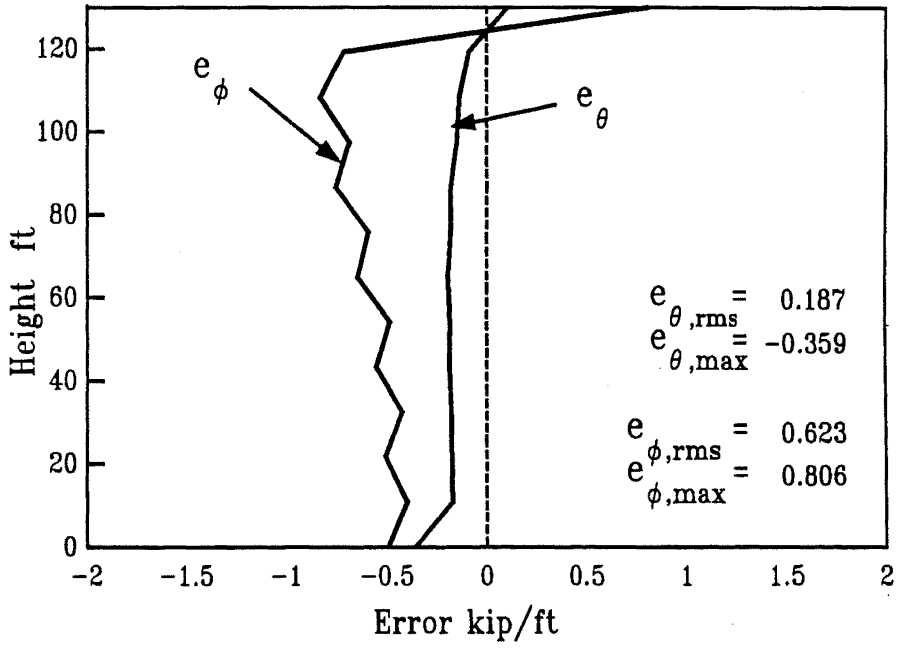

Fig. B

Error Distribution Along Height

Figure 3-24: Results for Structure C : Mesh size 12 * 12

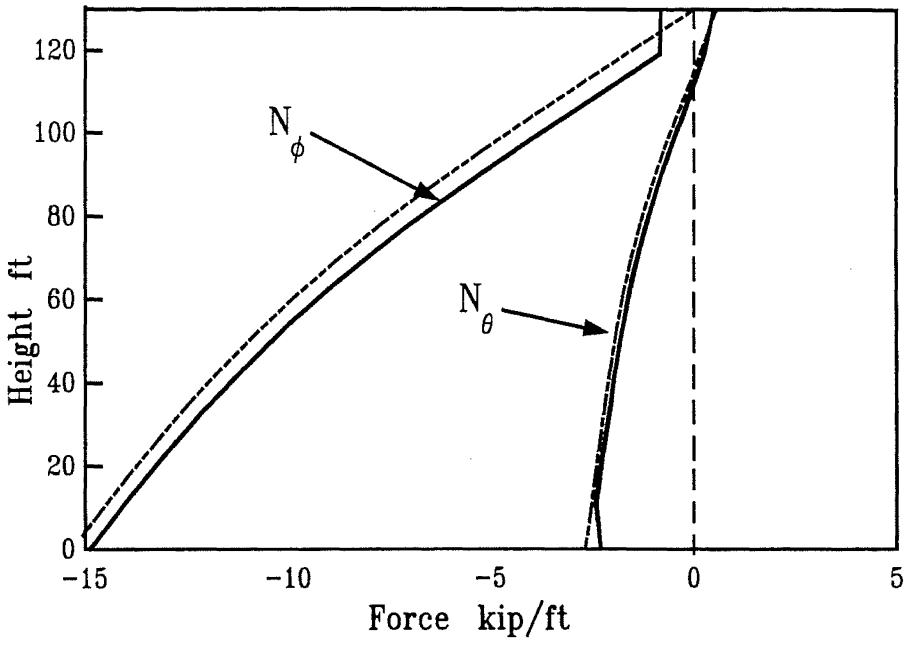

Fig. A

Shell Forces Along Height

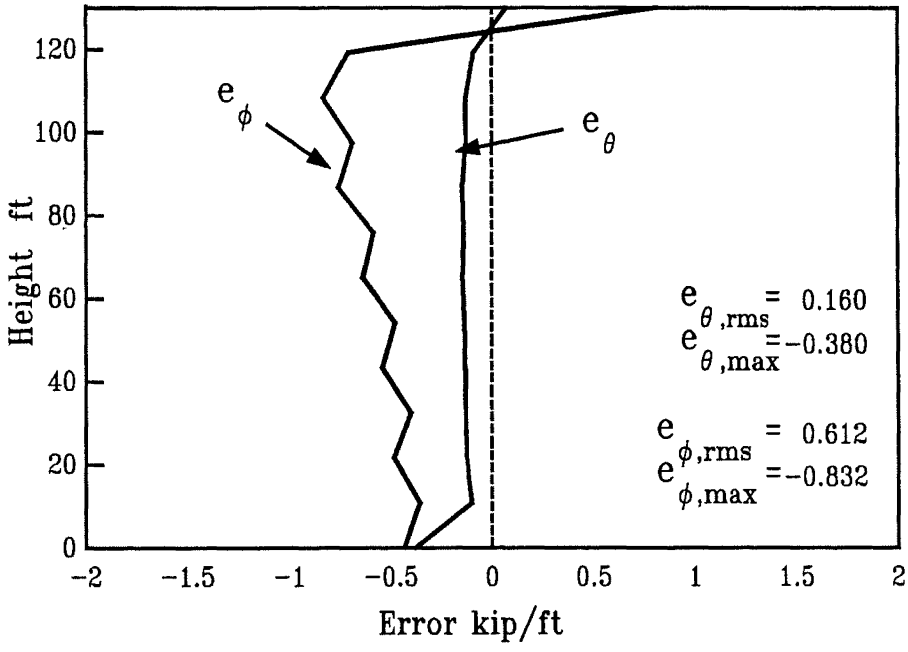

Fig. B

Error Distribution Along Height

Figure 3-25: Results for Structure C : Mesh size 16 * 12

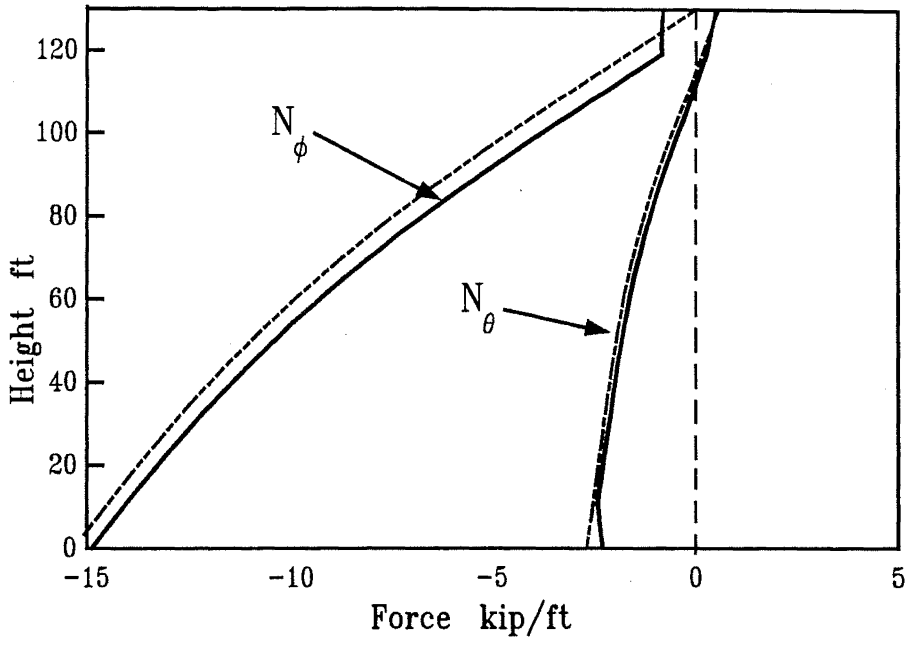

Fig. A

Shell Forces Along Height

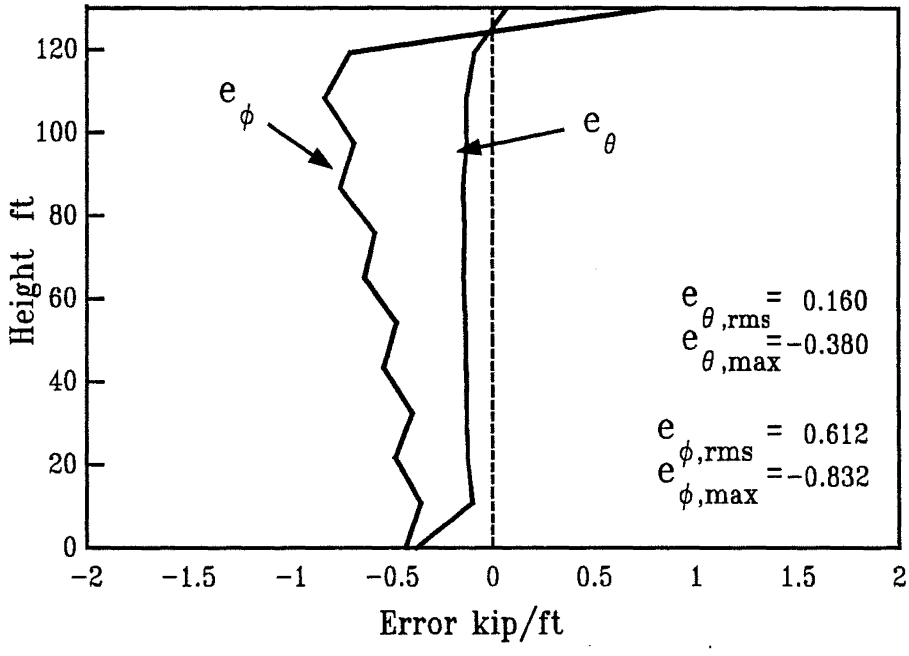

Fig. B

Error Distribution Along Height

Figure 3-26: Results for Structure C : Mesh size 20 * 12

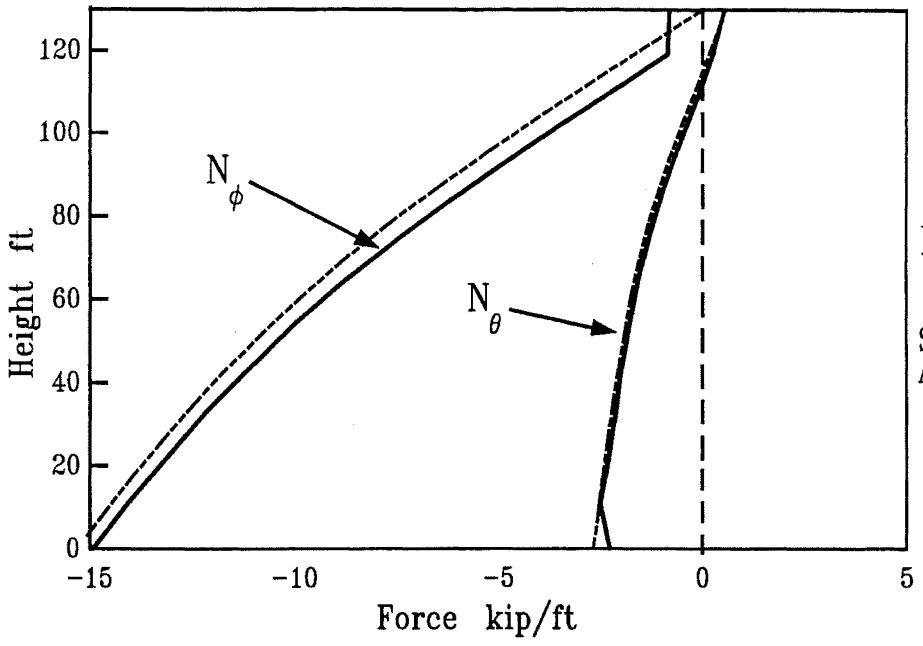

Fig. A

Shell Forces Along Height

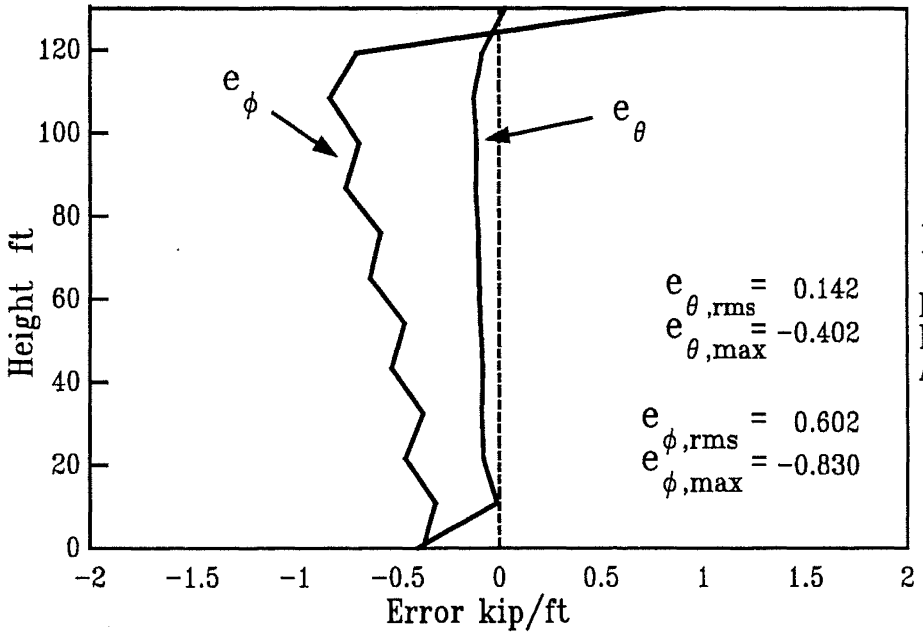

Fig. B

Error Distribution Along Height

Figure 3-27: Results for Structure C : Mesh size 30 * 12

Chapter 4
Discussion of Results

4.1 Effect of Mesh Fineness

The data presented in Chapter 3 is summarized in Fig.4-1 to 4-4. The variation of normalized RMS value of errors ($\bar{e}_\phi$ and $\bar{e}_\theta$) for different mesh fineness is shown. Fig.4-1 and 4-2 represent the error variation for different number of divisions in the finite element mesh along axial direction, while number of divisions in radial direction was kept constant at 24. Similarly Fig.4-3 and 4-4 represent the error variation for the different number of divisions along radial direction, while the axial direction divisions is fixed at 12.

4.1.1 Axial Direction

In the axial direction number of divisions in the FE mesh was varied from 6 to 15. Normalized RMS error in longitudinal shell force ($\bar{e}_\phi$) was found to range from 13.5% at 6 divisions to approximately 6% at 15 divisions (See Fig.4-1). As the mesh fineness in the axial direction was increased $\bar{e}_\phi$ gradually reduced. Above 12 divisions it remained fairly constant.

There was a wide variation of normalized RMS error in meridianal shell forces ($\bar{e}_\theta$). For Structure C, $\bar{e}_\theta$ was as high as 35% for low mesh fineness (6 div.) while for Structure B, it was as low as 7.5% for high mesh fineness (15 div.) (See Fig. 4-2). Generally $\bar{e}_\theta$ appeared to decrease for finer meshes.

In the hyperbolic cooling tower shells analyzed, 12 or higher number of divisions along the axial direction appeared to be necessary for an optimal solution.

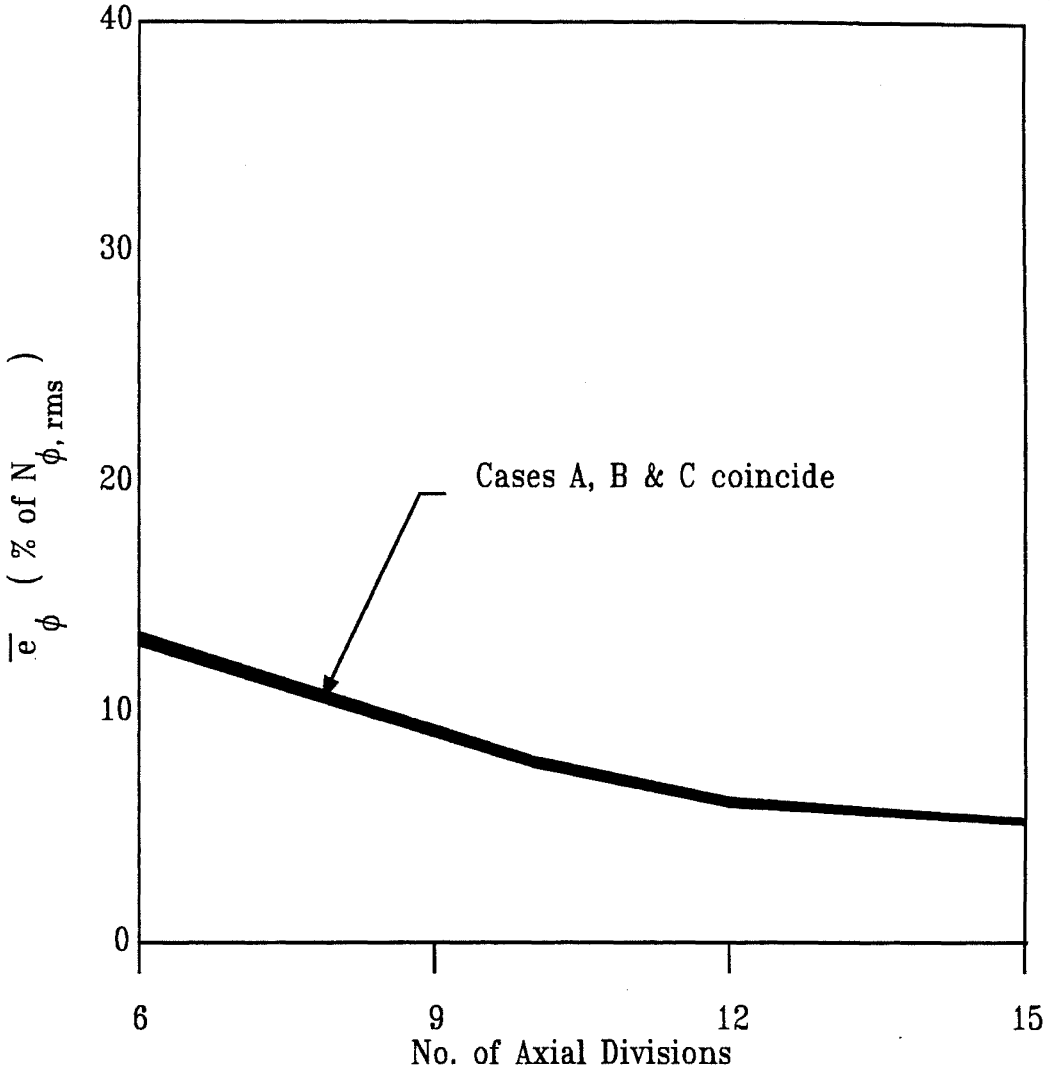

Figure 4-1: Relationship between Normalized RMS error in Longitudinal Direction and Longitudinal Mesh Fineness

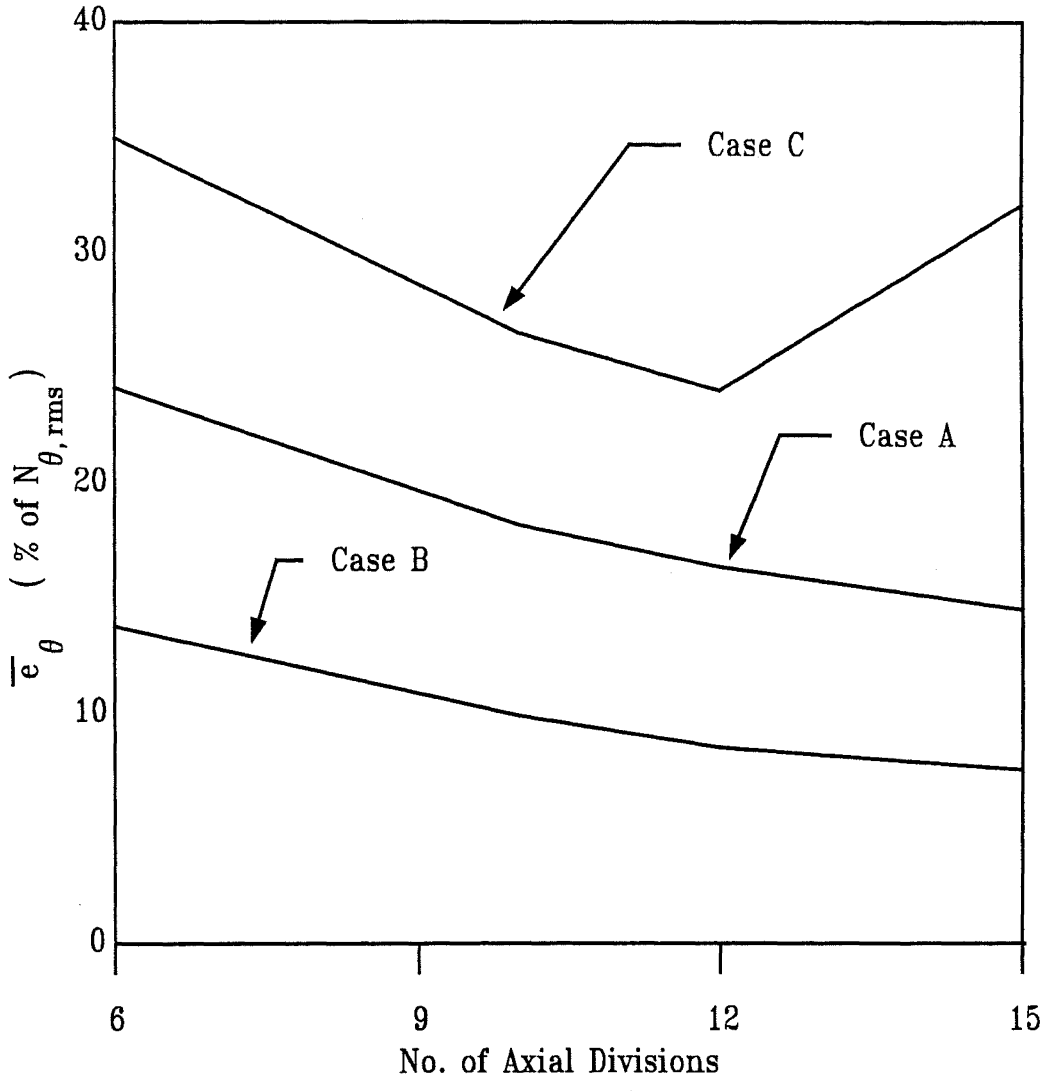

Figure 4-2: Relationship between Normalized RMS error in Meridianal Direction and Longitudinal Mesh Fineness

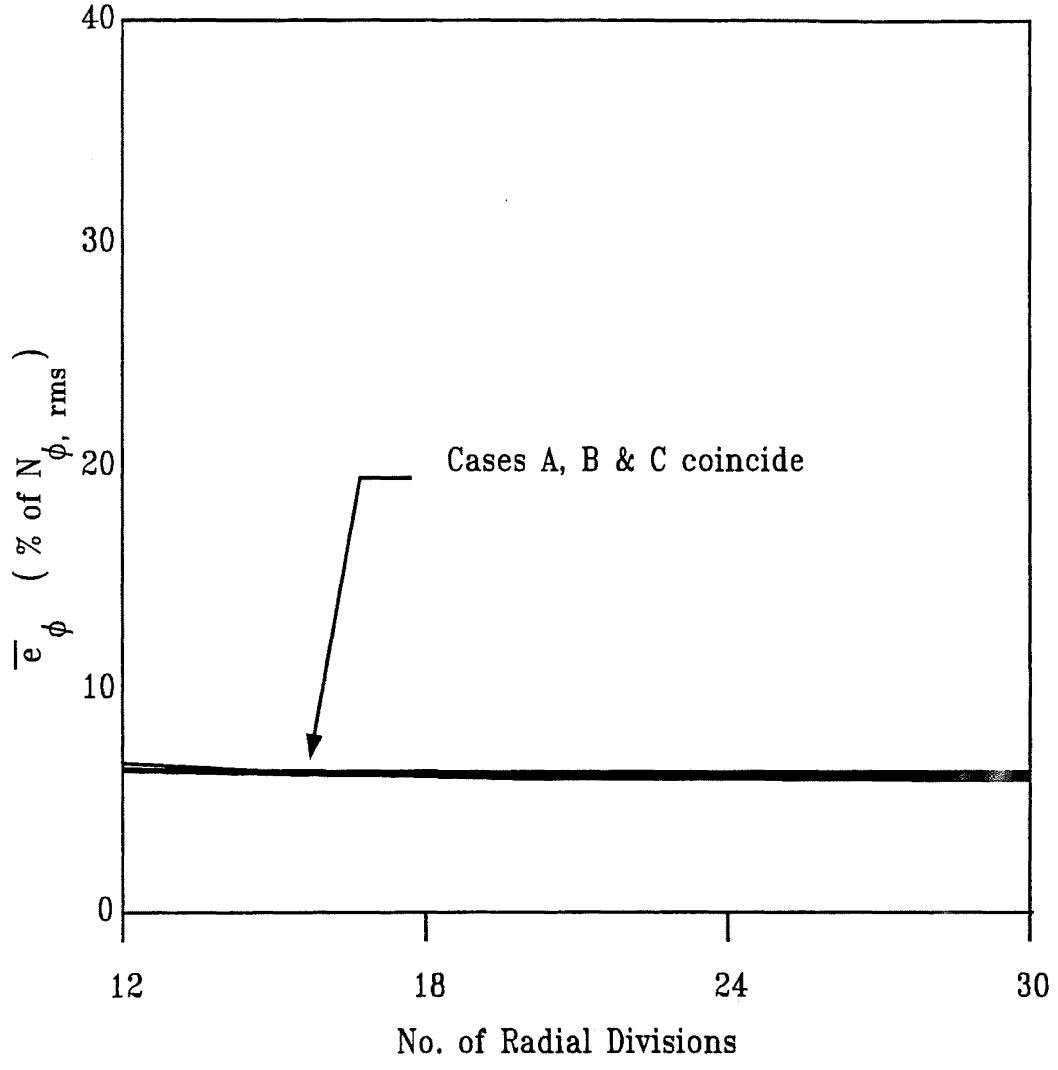

Figure 4-3: Relationship between Normalized RMS error in Longitudinal Direction and Meridianal Mesh Fineness

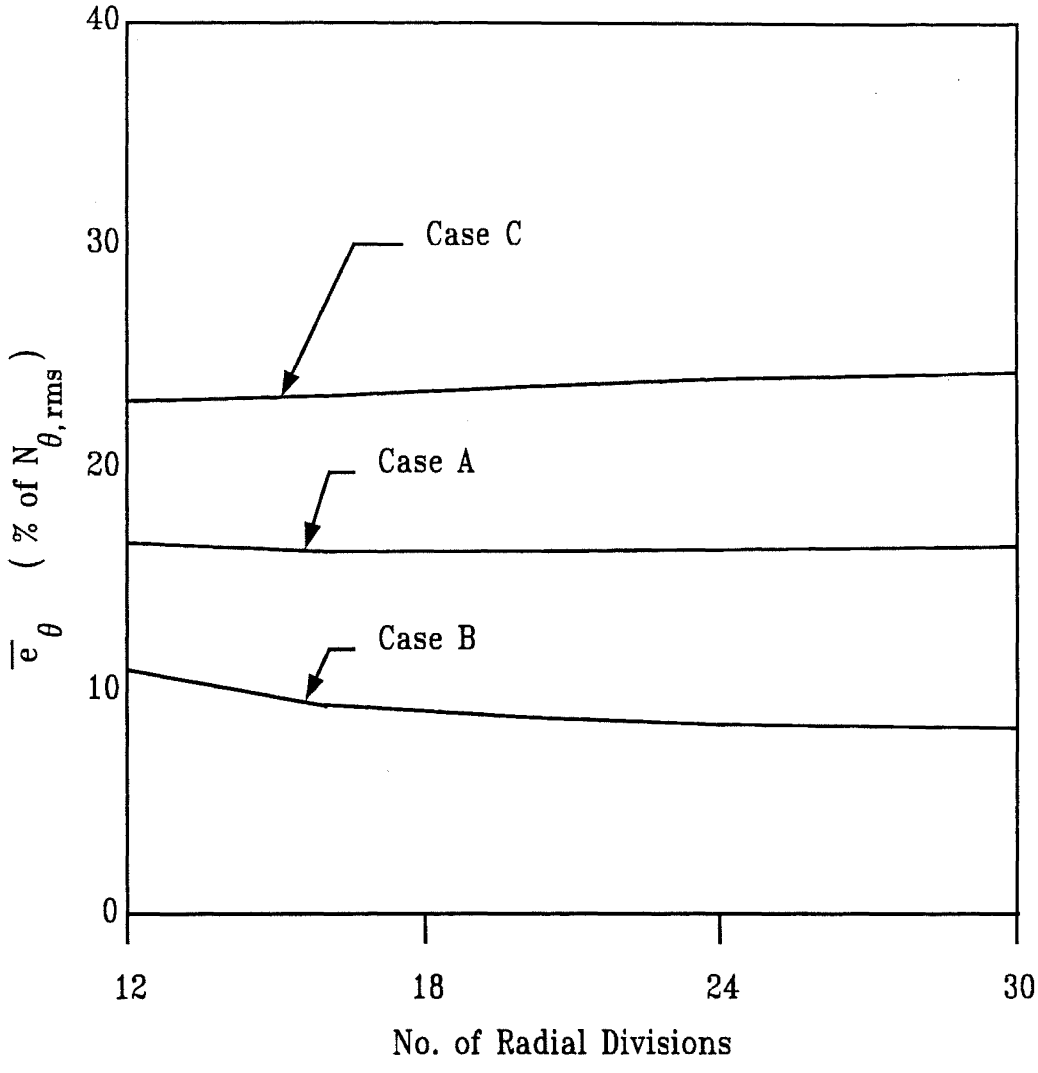

Figure 4-4: Relationship between Normalized RMS error in Meridianal Direction and Meridianal Mesh Fineness

4.1.2 Radial Direction

In the radial direction number of divisions in the FE mesh was varied from 12 to 30. Fineness of mesh in the radial direction appeared to have little effect on the accuracy of the solution. Curves showing the variation of normalized RMS errors for shell forces ($\bar{e}_\phi$ and $\bar{e}_\theta$) were more or less constant (See Fig.4-3 and 4-4). The level of error was pretty low for $\bar{e}_\phi$. While for $\bar{e}_\theta$ it was much higher in some cases.

This insensitivity of the accuracy of the solution to mesh fineness in the radial direction may be because there is no shell force gradient in the radial direction under the loading chosen (gravity loading, symmetric state of stress). For unsymmetric states of stress there would possibly be some difference in normalized RMS error levels for different mesh fineness in the radial direction.

From the available data on the hyperbolic cooling tower shells analyzed, 18 or higher number of divisions along the radial directions appeared to be a good choice. Though a lower number of divisions may not substantially raise the normalized RMS errors under the chosen loading, for a more general case, considering aspect ratio of the elements and different states of stress, at least 18 divisions in the radial direction is advised.

4.2 Effect of Shell Geometry

Three hyperbolic cooling tower shells (A, B and C) of different shapes were analyzed in this study. In general FE analysis of comparatively flat shells were more accurate than curved shells. From the results it was clear that $\bar{e}_\theta$ was very sensitive to the geometry. From Fig.4-2 and 4-4 it appears that there is a variation of 35% to 10% normalized RMS error in the estimate of N_θ depending

on the geometry. On the other hand, in the range of shells analyzed, normalized RMS error $\bar{e}_\phi$ did not show any dependency on the shell geometry. Note in Fig.4-1 and 4-3 the curves for all three structures coincide.

Table 4-1: Comparison of Geometric Parameters

Structure	a ft.	b ft.	A
A	30.0	70.0	66.8°
B	30.0	84.0	70.35°
C	30.0	56.0	61.82°

Table 4-1 shows the comparison of different geometric parameters of different shells. The costants a and b are used to define the shell generator curve. The angle A is the angle between the radial axis and the asymptotes of the meridianal hyperbola. The relations between these parameters can be found from simple geometry as,

$$A = \tan^{-1}(b/a)$$

From table 4-1 it is evident that comparatively small changes in the angle A, can substantially effect the level of normalized RMS error $\bar{e}_\theta$. In this range of shells $\bar{e}_\phi$ appear to be fairly insensitive to changes in the geometry.

Further parametric study is required to establish a numerical estimate of

FE mesh fineness required for a solution with acceptable level of errors for different geometries. However qualitatively it can be concluded that, for comparatively curved shells 24 * 12 or finer FE mesh is necessary, while for typical or flat shells 18 * 10 mesh fineness would be sufficient.

4.3 Aspect Ratio Variation

It is well known that aspect ratio of the elements may substantially affect the quality of FE analysis results. Aspect ratios close to unity are optimum for minimizing errors, while elements with aspect ratios greater than three may show significant error in analysis. In this study, aspect ratio is taken as,

$$\alpha = \frac{\text{Length of the longest side of element}}{\text{Length of the shortest side of element}}$$

. So aspect ratio is always greater than or equal to one.

Tables 4-2 and 4-3 present the aspect ratio variation for different meshes used in this study. From the tables it can be seen that the maximum aspect ratio in different meshes varied from 1.31 to 2.77 and was below 2 for most cases. The average aspect ratio varied from 1.09 to 2.54 and was below 1.5 for most cases. An aspect ratio of 1.0 is the best possible aspect ratio. These figures indicate that the elements in the FE meshes used in this analysis had excellent aspect ratio. So it can be safely assumed that the error analyses based on the results using these meshes were mostly free from the errors associated with elements having extreme aspect ratios.

Table 4-2: Maximum Aspect Ratio of Shell Elements

Mesh Size	Struct. A	Struct. B	Struct. C
24 * 6	2.76	2.75	2.77
24 * 10	1.66	1.65	1.66
24 * 12	1.38	1.38	1.38
24 * 15	1.49	1.36	1.68
12 * 12	2.39	2.18	2.7
16 * 12	1.79	1.63	2.02
20 * 12	1.43	1.31	1.62
24 * 12	1.38	1.38	1.38
30 * 12	1.73	1.72	1.73

Table 4-3: Average Aspect Ratio of Shell Elements

Mesh Size	Struct. A	Struct. B	Struct. C
24 * 6	2.49	2.54	2.43
24 * 10	1.47	1.51	1.44
24 * 12	1.26	1.26	1.28
24 * 15	1.11	1.09	1.14
12 * 12	1.77	1.69	1.88
16 * 12	1.33	1.27	1.41
20 * 12	1.18	1.15	1.23
24 * 12	1.26	1.26	1.28
30 * 12	1.52	1.56	1.48

4.4 Cost Effectiveness of Analysis

Cost of solving the problem is taken as the measure of the size of the model rather than number of nodes or other measures. Only the cost of executing the FE solution step is included in the cost estimate. Preprocessing costs (e.g. cost of running ADINA-IN) are not included.

The cost of running ADINA for each of the meshes analyzed is presented in Tables 3-1 to 3-3. The cost index is the actual cost in dollars for running ADINA for that mesh in batch mode and at off hours on a CDC-CYBER computer. The range of costs is from $0.52 for simpler meshes to $3.43 for the more sophisticated and refined meshes. This indicates that an analysis using finer meshes may cost 5 to 7 times the cost of using a simpler mesh. However these costs are so low that cost considerations do not play any part in choice of optimum meshes.

This analysis was limited to elastic material models and simple static loading. For nonlinear material models and dynamic analysis substantially more cost will be involved. Memory and computational effort (CPU time) limitations may actually limit the size of the model, rather than sheer cost. The ratio of costs between different meshsizes may be used as guidelines for estimating costs for meshes in other situations.

Chapter 5
Conclusions and Recommendations

5.1 Conclusions

The following conclusions about finite element (FE) analysis of hyperbolic cooling tower shells may be drawn from the data collected in this study.

- There is signicicant amount of error (as high as 20% to 35% in some cases) in the estimate of shell forces , especially for meridianal (hoop) forces.

- For symmetric states of stress, mesh fineness in the radial direction has little or no effect on the accuracy of the solution. However refining the mesh in the axial direction does improve the accuracy of the solution.

- The accuracy of longitudinal shell force (N_ϕ) estimate is quite good (approximately 10% or less error) in most choices of mesh and it is also fairly insensitive to the geometry in this class of shells in the range analyzed.

- The accuracy of meridianal shell force (N_θ) results is, however, very much dependent on the shape of the structure. Small changes in shape may significantly affect the accuracy of N_θ estimate. In the cases analyzed in this study the accuracy varied from 30% to 10% depending on the geometry of the shell for the same FE mesh.

- For a hyperbolic cooling tower of typical shape or flatter than typical shape, a mesh fineness of at least 18 * 10 is necessary for a reasonably good solution. However for more curved shells a

minimum mesh fineness of 24 * 12 is required. Even finer meshes may be necessary, in applications where a higher degree of accuracy is desired.

- Finite element analysis results typically underestimate (30% to 6% depending on the shell parameters) the compressive shell forces. Note that the distribution of errors over the height is not random and they show a substantial bias to the negative side in all the cases analyzed. Since most shells in practice are designed such that the shell surface is mostly in compression, this tendency of FE solutions produce unconservative estimates of shell forces.

- The aspect ratio of the elements in FE meshes used in this study are all less than 2.8 and mostly averages below 1.5 . Errors arising from extreme aspect ratios do not substantially affect the conclusions of this study.

- The cost of analysis is fairly low (typically $0.50 to $3.70 in batch mode in off hours on a CDC-CYBER machine) for elastic static analysis, even using fine meshes. The ratio of cost for analysis between the finest and crudest meshes considered in this study is between 5 to 7. Nonlinear material models and dynamic analysis would increase this estimate substantially.

5.2 Recommendations

To estimate the errors in FE analysis of the shell forces on hyperbolic cooling tower shells with better accuracy following areas may be researched.

- A thorough parametric study to quantify the relationship between errors and shape of the shell may be done.

- The choice of elements (e.g. 8 noded shell element) also significantly effect the accuracy of the solution. This is another possible area of research.

- To complement this study done under a symmetric state of stress, similar studies may be done on unsymmetric states of stress to find optimal mesh characteristics for minimizing error.

Similar studies on other shell structures (e.g. Cylindrical shells, Hyperbolic Paraboloids etc.) may be done to develop further understanding of the limitations of the accuracy of finite element method in thin shell structures. Development of such a knowledge base would ensure a more uniform treatment of FE analysis of thin shell structures and would prevent analysis errors from adversely affecting the structural performance.

5.3 Summary

Increased dependence on finite element modelling of structures in practice has made awareness of error potential of these analyses essential. Specifically this study indicates that FE analysis of hyperbolic cooling tower shells under gravity loading, may have substantial error and the analysis results may be unconservative in some cases. Error levels of unsymmetric states of stress would probably be higher.

Choice of appropriate FE mesh patterns, fineness and elements while forming the model, along with adoption of appropriate safety factors on the results when applied to design can be done to improve the reliability of FE results. This concern is more pertinent in case of shell structures, since FE analysis results of these structures is more error-prone. Further research is needed to develop guidelines for FE modelling of common structures, so that the analysis procedure may be more uniform and the results may be more reliable and error-free.

References

Ashfaque Chowdhury 1990
SIGNIFICANCE OF MESH-FINENESS IN ACCURACY OF FE ANALYSIS OF HYPERBOLIC COOLING TOWER SHELLS.. Technical Report LEHIGH/FL/354.548, Fritz Engineering Laboratory, Lehigh University.

P. Fazio and K. Gowri 1987
STRUCTURAL ANALYSIS SOFTWARE AND THE C PROGRAMMING LANGUAGE. Computers & Structures Vol. 25(No. 3):pp. 463-465.

Carl S. Grant and T. Y. Yang 1980
REFINED ANALYSIS OF THE SEISMIC RESPONSE OF COLUMN-SUPPORTED COOLING TOWER. Computers & Structures Vol. 11:pp. 225-231.

Nagesh R. Iyer and T. V. S. R. Appa Rao 1990
STUDIES ON STRESS CONCENTRATION AT SHELL-COLUMN JUNCTION OF HYPERBOLOID COOLING TOWERS. Computers & Structures Vol. 34(No. 2):pp. 191-202.

Christian Meyer 1987
FINITE ELEMENT IDEALIZATION FOR LINEAR STATIC AND DYNAMIC ANALYSIS OF STRUCTURES IN ENGINEERING PRACTICE. Technical Report, Task Committee on FE Idealization, ASCE.

G. S. Ramaswamy 1986
DESIGN AND CONSTRUCTION OF CONCRETE SHELL ROOFS. CBS Publishers & Distributors, Delhi-32, India.

Werner C. Rheinboldt 1985
ERROR ESTIMATES FOR NONLINEAR FINITE ELEMENT COMPUTATIONS. Computers & Structures Vol. 20(No. 1-3):pp. 91-98.

Mircea Soare 1967
APPLICATION OF FINITE DIFFERENCE EQUATION TO SHELL ANALYSIS. Pergamon Press., Oxford, London, UK.

Appendix A
Nomenclature

α	Aspect ratio of shell elements
δ	Shell thickness, (inch).
ϕ	Angle between principal radius r_1 and axis of revolution.
γ	Unit density of material, (kip/ft^3).
ν	Poisson's ratio.
θ	Angle in a plane perpendicular to axis of revolution between any point and radial axis in the same plane.
a	Shell constant, radius at origin (neck), (ft).
A	Angle between radial axis and asymptotes of meridianal hyperbola.
b	Shell constant , (ft).
E	Young's Modulus, (kip/ft^2).
$\mathbf{e}_\phi$	Error in longitudinal shell force at a point, (kip/ft).
$\overline{e}_\phi$	Normalized root mean square (RMS) error in longitudinal shell force over the entire shell, (%).
$\mathbf{e}_{\phi,\,\mathbf{rms}}$	Root mean squared (RMS) value of error in longitudinal shell force over entire shell, (kip/ft).
$\mathbf{e}_\theta$	Error in meridianal shell force at a point, (kip/ft).
$\overline{e}_\theta$	Normalized root mean square (RMS) error in meridianal shell force over the entire shell, (%).

$e_{\theta, rms}$	Root mean squared (RMS) value of error in meridianal shell force over entire shell, (kip/ft).
$f(\phi)$ or $f(z)$	Function used for numerical integration.
$I(z)$	Integrated function.
$N_{\phi\theta}$	In-plane Shear force in shell, (kip/ft)
N_{ϕ}	Shell force in the longitudinal direction, (kip/ft).
$N_{\phi, FE}$	Longitudinal shell force found by finite element (FE) analysis, (kip/ft).
$N_{\phi, rms}$	Root mean squared (RMS) value of longitudinal shell force over the entire shell, (kip/ft).
$N_{\phi, std}$	Longitudinal shell force found by standard solution, (kip/ft).
N_{θ}	Shell force in the meridianal direction, (kip/ft).
$N_{\theta, FE}$	Meridianal shell force found by finite element (FE) analysis, (kip/ft).
$N_{\theta, rms}$	Root mean squared (RMS) value of meridianal shell force over the entire shell, (kip/ft).
$N_{\theta, std}$	Meridianal shell force found by standard solution, (kip/ft).
q	Gravity loading on shell, (kip/ft^2).
r_0	Radius of shell at any height, (ft).
r_1	Maximum principal radius at any point on the shell, (ft).
r_2	Minimum principal radius at any point on the shell, (ft).
X	Body force along global x direction, (kip/ft^3).
Y	Body force along global y direction, (kip/ft^3).

$\mathbf{z}$	Coordinate along global z axis which coincides with the axis of revolution, (ft).
$\mathbf{z_{bottom}}$	z at the bottom of the shell, (ft).
$\mathbf{z_{top}}$	z at the top of the shell, (ft).
$\Delta\mathbf{z}$	Increment in z used in numerical integration, (ft).
$\mathbf{Z}$	Body force along global z direction, (kip/ft^3).

Appendix B
Standard Solution

B.1 Theoretical Background

In membrane theory for a shell of revolution, the differential equations of equilibrium can be derived as follows. (Soare, 1967) (See Fig. B-1)

$$\frac{\partial N_\theta}{\partial \theta} r_1 + \frac{\partial (N_{\phi\theta} r_0)}{\partial \phi} + N_{\theta\phi} r_1 \cos\phi + X r_0 r_1 = 0$$

$$\frac{\partial N_{\theta\phi}}{\partial \theta} r_1 + \frac{\partial (N_\phi r_0)}{\partial \phi} - N_\theta r_1 \cos\phi + Y r_0 r_1 = 0$$

$$\frac{N_\phi}{r_1} + \frac{N_\theta}{r_2} = -Z$$

For a symmetric loading case, $X = 0$ and $N_{\phi\theta} = N_{\theta\phi} = 0$. So the equations of equilibrium reduces to the following.

$$\frac{d(N_\phi r_0)}{d\phi} - N_\theta r_1 \cos\phi + Y r_0 r_1 = 0$$

$$\frac{N_\phi}{r_1} + \frac{N_\theta}{r_2} = -Z$$

From these equations, the solution for N_ϕ is found as,

$$N_\phi = \frac{1}{r_0 \sin\phi} \int_{\phi_0}^{\phi} f_\phi \, d\phi$$

$$f_\phi = r_0 r_1 (Y \sin\phi + Z \cos\phi)$$

For the case of gravity loading of intensity $\gamma\delta$, (γ : material density, and δ : shell thickness) the components of loading are,

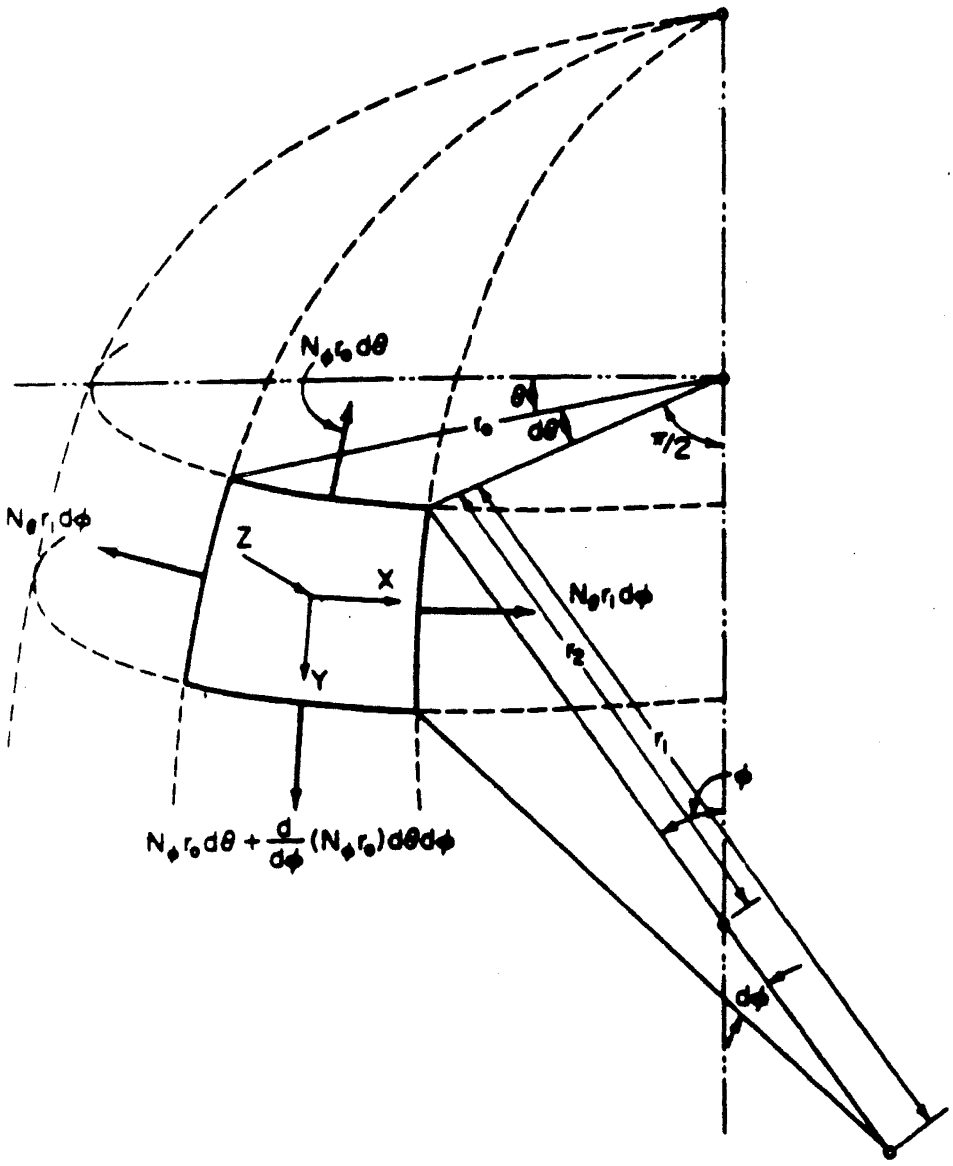

Taken from (Ramaswamy, 1986) Fig 14-7a, pp.366

Figure B-1: Typical Shell Element and Membrane Forces

$$Y = \gamma \delta \sin\phi$$

$$Z = \gamma \delta \cos\phi$$

Substituting and simplifying in the expression for $f(\phi)$,

$$f(\phi) = \gamma \delta r_0 r_1$$

Changing the independent variable from ϕ to height z, finally the following expressions may be derived.

$$f(z) = \gamma \delta r_2$$

$$I(z) = \int_{z_{top}}^{z} f(z)\, dz$$

$$N_\phi = -\frac{I(z)}{r_0 \sin\phi}$$

The meridianal forces are found as follows.

$$N_\theta = - Z r_2 - N_\phi \frac{r_2}{r_1}$$

B.2 Numerical Analysis

Dimensions and material properties of the structure being known, the shape properties of the shell at any given height can be found from geometric consideration. To find the forces, numerical integration of $I(z)$ along the height is done. Once $I(z)$ is known finding the forces at that z, is trivial.

From geometrical considerations,

$$r_0 = a\sqrt{1 + (z/b)^2}$$

$$\phi = \tan^{-1}\left(\frac{b\, r_0}{a\sqrt{r_0^2 - a^2}}\right)$$

$$r_2 = \frac{r_0}{\sin\phi}$$

$$Z = \gamma\,\delta\cos\phi$$

For Numerical Integration the shell is divided into n (n = 180 in this study) 'slices' of equal height of Δz. Then following equation derived from the trapezium rule, is used at m^{th} division.

$$I_m = \frac{\Delta z}{2}(f_{m-1} + 2f_m + f_{m+1}) + I_{m-2}$$

Using this scheme numerical integration of $f(z)$ over the height is done. The numbering of divisions starts at the top of the shell and increases towards the bottom.

Knowing numerical values of material properties and r_0, r_1, r_2, ϕ, Z and $I(z)$, numerical values of forces at any given z is found by substituting in the appropriate equations.